Cell. Mol. Life Sci. (2018) 75:335–354
https://doi.org/10.1007/s00018-017-2632-8

Cellular and Molecular Life Sciences

ORIGINAL ARTICLE

Pathogenic mutation in the ALS/FTD gene, *CCNF*, causes elevated Lys48-linked ubiquitylation and defective autophagy

Albert Lee[1,2] · Stephanie L. Rayner[1,3] · Serene S. L. Gwee[1] · Alana De Luca[1] · Hamideh Shahheydari[1] · Vinod Sundaramoorthy[1] · Audrey Ragagnin[1] · Marco Morsch[1] · Rowan Radford[1] · Jasmin Galper[1] · Sarah Freckleton[1] · Bingyang Shi[1] · Adam K. Walker[1] · Emily K. Don[1] · Nicholas J. Cole[1] · Shu Yang[1] · Kelly L. Williams[1] · Justin J. Yerbury[4] · Ian P. Blair[1] · Julie D. Atkin[1,5] · Mark P. Molloy[2,3] · Roger S. Chung[1]

Received: 13 March 2017 / Revised: 29 July 2017 / Accepted: 23 August 2017 / Published online: 29 August 2017

Abstract Amyotrophic lateral sclerosis (ALS) and frontotemporal dementia (FTD) are fatal neurodegenerative disorders that have common molecular and pathogenic characteristics, such as aberrant accumulation and ubiquitylation of TDP-43; however, the mechanisms that drive this process remain poorly understood. We have recently identified *CCNF* mutations in familial and sporadic ALS and FTD patients. *CCNF* encodes cyclin F, a component of an E3 ubiquitin–protein ligase ($SCF^{cyclin\ F}$) complex that is responsible for ubiquitylating proteins for degradation by the ubiquitin–proteasome system. In this study, we examined the ALS/FTD-causing p.Ser621Gly (p.S621G) mutation in cyclin F and its effect upon downstream Lys48-specific ubiquitylation in transfected Neuro-2A and SH-SY5Y cells. Expression of mutant cyclin F^{S621G} caused increased Lys48-specific ubiquitylation of proteins in neuronal cells compared to cyclin F^{WT}. Proteomic analysis of immunoprecipitated Lys48-ubiquitylated proteins from mutant cyclin F^{S621G}-expressing cells identified proteins that clustered within the autophagy pathway, including sequestosome-1 (p62/SQSTM1), heat shock proteins, and chaperonin complex components. Examination of autophagy markers p62, LC3, and lysosome-associated membrane protein 2 (Lamp2) in cells expressing mutant cyclin F^{S621G} revealed defects in the autophagy pathway specifically resulting in impairment in autophagosomal–lysosome fusion. This finding highlights a potential mechanism by which cyclin F interacts with p62, the receptor responsible for transporting ubiquitylated substrates for autophagic degradation. These findings demonstrate that ALS/FTD-causing mutant cyclin F^{S621G} disrupts Lys48-specific ubiquitylation, leading to accumulation of substrates and defects in the autophagic machinery. This study also demonstrates that a single missense mutation in cyclin F causes hyper-ubiquitylation of proteins that can indirectly impair the autophagy degradation pathway, which is implicated in ALS pathogenesis.

Keywords Ubiquitylation · Phosphorylation · CCNF · Cyclin F · Amyotrophic lateral sclerosis · Frontotemporal dementia · Motor neuron disease

Electronic supplementary material The online version of this article (doi:10.1007/s00018-017-2632-8) contains supplementary material, which is available to authorized users.

✉ Albert Lee
albert.lee@mq.edu.au

1 Centre for Motor Neuron Disease Research, Department of Biomedical Sciences, Faculty of Medicine and Health Sciences, Macquarie University, 2 Technology Place, North Ryde, NSW 2109, Australia

2 Australian Proteome Analysis Facility, Macquarie University, Research Park Drive, North Ryde, NSW 2109, Australia

3 Department of Chemistry and Biomolecular Sciences, Faculty of Science and Engineering, Macquarie University, Research Park Drive, North Ryde, NSW 2109, Australia

4 Illawarra Health and Medical Research Institute, School of Biological Sciences, University of Wollongong, Northfields Avenue, Wollongong, NSW 2522, Australia

5 Department of Biochemistry and Genetics, La Trobe Institute for Molecular Science, Melbourne, VIC 3086, Australia

Introduction

Amyotrophic lateral sclerosis (ALS) is characterised by the progressive death of motor neurons in the brain and spinal cord leading to paralysis and muscle degeneration. We identified pathogenic mutations in a new ALS/FTD gene, *CCNF*, in both familial and sporadic ALS/FTD patients [1]. More recently, we have shown that expression of a pathogenic

mutation in the *CCNF* gene in zebrafish caused motor neuron axonopathy, consisting of shortened primary motor axons that led to increased cell death in the spinal cord and an aberrant motor phenotype [2]. The *CCNF* gene encodes the protein cyclin F, a component of an Skp1-Cul1-F-box (SCF) E3 ubiquitin–protein ligase complex that is an integral part of a cell's protein recycling system that ubiquitylates unnecessary and damaged proteins for degradation by the proteasome [3].

Protein degradation is an essential cellular process that is carried out by two major intracellular protein degradation pathways: the ubiquitin–proteasome system (UPS) and autophagy. Ubiquitylation is carried out in three main steps: activation by E1s, ubiquitin conjugation by E2s, and substrate ligation by E3s. The result of this sequential cascade is the covalent attachment of ubiquitin-to-lysine residues on proteins, with the use of different lysine residues in ubiquitin resulting in specific chain types that direct the tagged proteins to different functional outcomes. Distinct polyubiquitylation linkages on substrates target their destruction via different proteolytic pathways. For example, Lys48-ubiquitylated substrates are degraded by the proteasome, and those that are Lys63-ubiquitylated are degraded by autophagy [4, 5]. However, the cell's compensatory pathways allow both Lys48- and Lys63-ubiquitylated substrates to be degraded by either UPS and/or autophagy pathways via different mechanisms [6–11]. One example is the adaptor protein, p62/SQSTM1, which binds Lys63-ubiquitylated substrates and sequesters them for autophagic degradation, but upon casein kinase II-mediated phosphorylation at Ser403, sequestosome-1 (p62/SQSTM1) switches its binding to target Lys48-ubiquitylated substrates for autophagy [6].

Autophagy is a degradative process by which redundant and dysfunctional components are catabolized by lysosomes by either (1) engulfing and delivering cytosolic components in bulk to lysosomes (macroautophagy), or (2) direct engulfment of small volumes of cytosolic substrates by lysosomes (microautophagy), or (3) selecting substrates containing a pentapeptide motif (KFERQ) bound to chaperone complexes that are translocated to the lysosome (chaperone-mediated autophagy). Defective autophagy has been associated with pathological mutations of several ALS and FTD-linked genes including *SOD1* [12], p62/*SQSTM1* [13], *FUS* [14, 15], *TARDBP* [16], *DCTN* [17, 18], *VCP* [19], *TBK1* [20, 21], *OPTN* [22–24], and *CHMP2B* [25] suggesting that such defects play a causative role in ALS pathogenesis. Furthermore, the proteins encoded by many of these ALS/FTD genes (*SQSTM1, VCP, TBK1, OPTN,* and *CHMP2B*) are also components of the autophagic machinery. In addition, genetic ablation of Atg5 and Atg7, proteins that are required for autophagosome formation, in mice led to motor deficits and spontaneous accumulation of ubiquitylated protein inclusions in motor neurons, further suggesting that compromised autophagy contributes to ALS pathogenesis [26, 27]. Impairments to any of the multitude of steps in the autophagy process can lead to defective autophagic flux and vesicle trafficking, particularly in neurons, where retrograde transport of autophagosomes over relatively long distances is required to fuse with the lysosome in the cell body [28].

In this study, we identify differences in Lys48-ubiquitylated proteins in cells expressing wild-type cyclin F and ALS/FTD pathogenic mutant cyclin F^{S621G}. Using a combination of Lys48-specific immunoprecipitations and mass spectrometry profiling, we demonstrate that expression of cyclin F^{S621G} leads to accumulation of Lys48-ubiquitylated proteins that cluster within essential cellular pathways including autophagy. Accordingly, we show that autophagosomal formation and lysosomal fusion are significantly impaired in neuronal-like cells expressing mutant cyclin F^{S621G} compared to wild-type cyclin F. These findings provide the first mechanistic insight into how a disease-causing mutation in cyclin F contributes to defects in protein degradation pathways that may underlie the pathogenesis of ALS/FTD.

Methods

Reagents and antibodies

All chemicals and reagents were of the highest grade and obtained from Sigma-Aldrich unless otherwise stated. The antibodies used in this study include: rabbit anti-Lys48 ubiquitin clone Apu2 (catalog #05-1307, Millipore, MA, USA), rabbit anti-Lys63 ubiquitin clone Apu3 (catalog #05-1308, Millipore, MA, USA), mouse anti-ubiquitin (FK2) (catalog #BML-PW8810, Enzo Life Sciences, NY, USA), rabbit anti-profilin (catalog #3237, Cell Signaling Technology, MA, USA), rabbit anti-mCherry (catalog #NBP2-43727, Novus Biologicals, CO, USA), rabbit anti-p62/SQSTM1 (catalog #5114, Cell Signaling Technology, MA, USA and catalog #P0067, Sigma-Aldrich, MO, USA), rabbit anti-microtubule-associated protein 1A/1B-light chain 3 (LC3) (catalog #NB100-2220, Novus Biologicals, CO, USA), rabbit anti-Lamp2a (catalog #ab18528, Abcam, Cambridge, UK), mouse anti-Gapdh (catalog #NB300-221, Novus Biologicals, CO, USA), mouse anti-FLAG clone M2 (catalog #F3165, Sigma-Aldrich, MO, USA), and pre-immune normal rabbit IgG (catalog #sc-2027, Santa Cruz Biotechnology, TX, USA).

Cell culture and transfection

Neuro-2A, SH-SY5Y, or HEK293 cells were plated at 1×10^6 cells in 100 mm plates and maintained in DMEM (Sigma-Aldrich, MO, USA) supplemented with 10%

heat-inactivated fetal bovine serum (FBS) (Sigma-Aldrich, MO, USA) and 1% antibiotics (100 mg/mL streptomycin and 100 U/mL penicillin) (Sigma-Aldrich, MO, USA) in a 37 °C heat-jacket humidified incubator with 5% CO_2. Following 48 h of growth, Neuro-2A, SH-SY5Y or HEK293 cells were transfected with cDNA constructs as previously described [1]. Neuro-2A cells were used for all proteomics analysis, immunoprecipitations and immunoblotting analysis. SH-SY5Y and HEK293 cells were used for immunoblot analysis for autophagy markers (Lamp2a, LC3, and p62/SQSTM1). SH-SY5Y cells were used to measure the level of autophagosome fusion by confocal microscopy. Primary fibroblast cultures were maintained and written consent and human research ethics are previously described [29].

Cell lysis and immunoprecipitation

Transfected Neuro-2A cells were lysed with probe sonication (10 s, Setting 3, Branson Sonifier 450) in extraction buffer (1% (v/v) Nonidet P-40 in Tris-buffered saline (TBS) containing 2 mM EDTA), 10 mM *N*-ethylmaleimide and complete protease inhibitor cocktail and phosSTOP (Roche, WI, USA). Cellular debris was pelleted at 14,000×*g* (30 min at 4 °C). Typically, 2 µg of antibody per 500 µg of protein extract was used for immunoprecipitations. Protein A/G magnetic beads (Catalog #88802, Pierce Biotechnology, IL, USA) were used to capture the antibody:protein complex. Immunoprecipitation mixtures were washed with extraction buffer and then either resuspended in 1× LDS buffer with 50 mM DTT, and heated at 95 °C for 10 min for western blot analyses or washed in PBS, eluted with 0.2 M glycine pH 2.5 and neutralised with 0.2 M Tris pH 9.0 for in-solution trypsin digestion and LC–MS/MS analyses. A pre-immune control IgG immunoprecipitation was carried out in triplicate, and the non-specific proteins identified from this analysis were excluded from the collection of identified proteins from mCherry-transfected cells. All cell lysis and immunoprecipitations procedures were carried out on transfected Neuro-2A cell lines from different passages.

SDS PAGE and western blotting analysis

Denatured proteins (15 µg) were separated on 4–12% Bis–Tris pre-cast gels according to manufacturer's instructions. SDS PAGE-separated proteins were transferred onto nitrocellulose membranes using the Bio-Rad Turbo Transfer apparatus (13 V, 1.3 A for 7 min or 25 V, and 2.5 A for 10 min). Blots were incubated with primary antibodies (1:1000) in 3% (w/v) bovine serum albumin (BSA) in phosphate-buffered saline with 0.05% (v/v) Tween-20 (PBS/T) overnight at 4 °C. After incubation, membranes were incubated with fluorescently labelled IRDye 800CW Goat Anti-Rabbit IgG or IRDye 700CW Goat Anti-mouse IgG secondary antibodies (1:15,000). Proteins were imaged using an Li-Cor Odyssey imaging system at the appropriate wavelength. Densitometry analysis was conducted using the ImageJ software (v1.47; National Institute of Health) [30] and statistics were conducted using Microsoft Excel and GraphPad Prism. Graphs were made using GraphPad Prism and Microsoft Excel.

Immunofluorescence microscopy and co-localization analysis

Neuro-2A cells were plated at 1.6×10^5 cells/well in 6-well plates with glass coverslips pre-coated with poly-L-lysine (catalog #P4707, Sigma-Aldrich, MO, USA). Following 48 h of growth, cells were transfected with 1.3 µg of DNA and allowed to incubate as described above. Cells were washed with sterile PBS, fixed with 4% (v/v) paraformaldehyde, and washed with PBS. Fixed cells were permeabilized with PBS containing 0.2% (v/v) Triton-X-100 for 10 min, before incubating with blocking solution (1% (w/v) BSA in PBS/T and 0.2 M glycine). The coverslips were incubated with anti-Lys48 ubiquitin in 1% (w/v) BSA in PBS/T (1:100) overnight at 4 °C, washed with PBS, and further conjugated with secondary antibody (1:250, anti-rabbit Alexa Fluor-488, Molecular Probes) for 1 h at RT. The coverslips were mounted in ProLong® Gold antifade Mountant with DAPI (Life Technologies) and imaged on Leica TCS SP8 Confocal Microscope. The level of co-localization was calculated using the iMaris software (Bitplane) and analysed based on the degree of overlapped signals between the proteins of interest via the threshold Mander's coefficient [31]. The Mander's correlation coefficient measures the degree of overlapping between signals captured in the two channels.

Autophagic flux measurements by immunofluorescence microscopy

Human neuroblastoma SH-SY5Y cells were seeded in 24-well plates containing 13-mm round coverslips and maintained in complete DMEM. Cells were maintained in a humidified 37 °C incubator with 5% CO_2. Cells were co-transfected transiently with pcDNA3.1-FLAG-$CCNF^{WT}$, pcDNA3.1-FLAG-$CCNF^{S621G}$ or pcDNA3.1 vector, and mCherry-EGFP-LC3 deposited by Dr. Jayanta Debnath (Addgene plasmid # 22418) [32] using Lipofectamine 2000 (Life Technologies; 11668) according to the manufacturer's instructions. After 42 h post-transfection, cells were serum-starved for 6 h to induce autophagy followed by fixation in 4% paraformaldehyde in phosphate-buffered saline (PBS) for 10 min. As a positive control, untransfected and co-transfected cells with FLAG-*CCNF* and mCherry-EGFP-LC3 were also treated with 100 nM bafilomycin (BFA) for 4 h and measured according to Klionsky et al. [33]. Cells were

washed three times with PBS after each step and permeabilised with 0.1% Triton-X-100, then blocked with 1% bovine serum albumin (Sigma) in PBS for at least 1 h at room temperature. Cells were then incubated with anti-FLAG (1:250, Sigma) antibody overnight and washed three times with PBS. Secondary Alexa Fluor-647 conjugated anti-mouse (1:1000, Life Technologies) was incubated for 1 h at room temperature, and then, cells were washed two times with PBS. Coverslips were mounted in fluorescence mounting medium (DAKO, North Sydney, NSW, Australia). Zeiss LSM 880 laser scanning microscope was used to acquire images (Carl Zeiss, Oberkochen, Germany). Images were collected using a 100×/1.4 Plan-Apochrome oil objective lens as sequential scans using Zeiss LSM 880 inverted confocal microscope. In dual-channel imaging, photomultiplier sensitivities and offsets were set to a level at which bleed-through effects from one channel to another were negligible. The Z-stack images were generated using a constant Z-stack interval. Green fluorescence was detected using an Argon laser, red fluorescence was detected using a DPSS 561-10 laser, and far red fluorescence was detected using a HeNe633 laser. All images were processed using the Zen imaging software. In a merged image, double-tagged mCherry-GFP-LC3, which appears that yellow and mCherry in red were counted per cell. Twenty-five cells were scored in each experiment and all experiments were performed in triplicate. Only single cells expressing both FLAG and mCherry-GFP-LC3 were selected for analysis. The bar graph shows the average percentage of autophagosomes (yellow) and autolysosmes (red) of total LC3-labelled vesicles.

E3 ligase activity assay

E3 ligase activity was determined using the E3LITE Customisable Ubiquitin Ligase ELISA Kit (LifeSensors, PA, USA) as per manufacturer's instructions. UBE2D3 was selected as the E2 enzyme and Lys48–ubiquitin was selected as the ubiquitin substrate. Briefly, mCherry-only vector, mCherry–cyclin F or pre-immune rabbit control IgG was immunoprecipitated from transfected Neuro-2A cells as described above. Protein A/G beads were washed (3×) in 100 mM Tris–HCl (pH 8.0), 10 mM $MgCl_2$ and resuspended in 25 µl in assay buffer (100 mM Tris–HCl, 10 mM $MgCl_2$, 0.2 mM DTT, pH 8.0). Immunoprecipitated mCherry, mCherry-cyclin F, and pre-immune rabbit control IgG were then added to wells containing the enzyme cocktail (E1 activating enzyme, E2 conjugating enzyme UBE2D3, and recombinant Lys48–ubiquitin). Each ligase reaction was activated by the addition of ATP (0.4 mM) and incubated at room temperature for 30 min. Each well was washed with PBS/T (3×), incubated with detection solution 1 for 60 min at RT, and followed by incubation with streptavidin-HRP for 60 min at room temperature. Luminescence was measured on a FLUOstar OPTIMA reader (BMG Labtech).

Trypsin digestion and LC–MS/MS

Immunoprecipitated proteins from transfected Neuro-2A cell lysates were reduced and alkylated with 10 mM DTT and 55 mM iodoacetamide (IAA), respectively, and digested with trypsin (1:50 enzyme:protein) overnight at 37 °C. The digestion was inactivated by the addition of 2 µL of formic acid. Tryptic peptides were desalted on a pre-equilibrated C_{18} Sep-Pak cartridge and eluted in 90% (v/v) ACN, 0.1% (v/v) formic acid, and dried under vacuum centrifugation.

Peptide fractions were separated on a nanoLC system (Thermo) employing a 90 min gradient (5–40% v/v acetonitrile, 0.1% v/v formic acid for 85 min followed by 90% v/v acetonitrile, and 0.1% v/v formic acid for 5 min) with a flow rate of 300 nL/min. The peptides were eluted and ionized into either an Orbitrap Velos or Q-Exactive mass spectrometer (Thermo). The electrospray source was fitted with an emitter tip 10 µm (New Objective, Woburn, MA, USA) and maintained at 2.0 kV electrospray voltage. Precursor ions were selected for MS/MS fragmentation using a data-dependent "Top 10" method operating in FT-FT acquisition mode with CID or HCD fragmentation. IT-MS and FT-MS on the Orbitrap Velos were carried out with a survey scan range between m/z 350 and1800 Da with MS/MS threshold of 500 ions for CID, and MS/MS threshold of 5000 ions for HCD, with an isolation width of 2.0 Da and normalised collision energy of 35%.

FT-MS analysis on the Q-Exactive was carried out with a 35,000 resolution and an AGC target of 1×10^6 ions in full MS; and MS/MS scans were carried out at 17,500 resolution with an AGC target of 2×10^5 ions. Maximum injection times were set to 120 and 60 ms, respectively. The ion selection threshold for triggering MS/MS fragmentation was set to 25,000 counts and an isolation width of 1.9 Da was used to perform HCD fragmentation with normalised collision energy of 30%.

Spectra files were processed using the Proteome Discoverer 1.4 software (Thermo) incorporating the Mascot search algorithm (Matrix Sciences, UK). Peptide identifications were determined using a 30-ppm precursor ion tolerance and a 0.8-Da MS/MS fragment ion tolerance for IT-MS and CID fragmentation, or 10-ppm precursor ion tolerance and a 0.05-Da MS/MS fragment ion tolerance for FT-MS and HCD fragmentation. Carbamidomethylation modification of cysteines was considered a static modification, while oxidation of methionine, deamidation of asparagine and glutamine, GlyGly residues on lysine, and acetyl modification on N-terminal residues were set as variable modifications allowing for maximum three missed cleavages. The data were processed through percolator for estimation of

false discovery rates. Protein identifications were validated employing a q value of 0.01, a minimum of two peptides and protein identification in at least three of the five replicates was used as additional filtering criteria. The data have been deposited to the ProteomeXchange with identifier PXD002011 (Username: reviewer04404@ebi.ac.uk; Password: wGNmnf1g).

Gene ontology annotation and ingenuity analysis

Gene ontology (GO) annotations were analysed using the DAVID Bioinformatics Resources software (http://david.abcc.ncifcrf.gov/). Each identifier was mapped from non-redundant Protein Information Resource (PIR) databases. InterPro annotations of domain and motif information were obtained in a sequencewise manner and collated together with annotations retrieved from Gene Ontology Mapping.

Ingenuity Analysis® was used to interrogate the filtered lists of immunoprecipitated Lys48-ubiquitylated proteins. The IPA core analysis employed the Ingenuity Knowledge Base references set to identify direct and indirect relationships in mouse cell lines only composing of 35 molecules per network with each analysis composing of 50 networks based on the IPA content version 14855783 (release date April 5, 2013). Protein networks were extracted using the IPA software based on the core analysis of the filtered data set.

Results and discussion

We recently identified a mutation in the *CCNF* gene (p.S621G) in a large Australian family with ALS and FTD [1], and expression of the cyclin F^{S621G} mutant protein in zebrafish caused motor neuron axonopathy. This consisted of shortened primary motor axons that led to increased cell death in the spinal cord and an aberrant motor phenotype [2]. In this previous study, we identified by label-free quantitative proteomics increased expression of caspase-3 in transfected Neuro-2A cells expressing mutant cyclin F^{S621G} compared to the wild type. We verified this finding by transient overexpression of human *CCNF* in zebrafish embryos and confirmed increased levels of cleaved (activated) caspase-3 and increased cell death in the spinal cord of zebrafish-expressing mutant cyclin F^{S621G} [2]. However, the underlying molecular mechanism by which cyclin F^{S621G} triggers apoptosis is unknown.

To address this issue, we have investigated whether the S621G mutation alters the ubiquitylation activity of cyclin F. Given the role of cyclin F as the substrate recognition subunit of the $SCF^{(cyclin\ F)}$ E3 ubiquitin ligase complex, we previously observed increased global levels of ubiquitylated proteins [1]. We predict that the S621G mutation directly alters the ubiquitylation activity of cyclin F^{S621G}. Hence, in this study, we examined the specific E3 ligase activity of immunoprecipitated wild type and mutant cyclin F^{S621G} and whether different classes of proteins were Lys48-ubiquitylated. Accordingly, we report that expression of cyclin F^{S621G} resulted in specific increase of Lys48-ubiquitylated proteins, but not Lys63-ubiquitylated proteins. Furthermore, we have used a proteomics workflow to identify and compare the different subsets of Lys48-ubiquitylated proteins from neuronal-like cells expressing cyclin F^{WT} and cyclin F^{S621G}. We identified Lys48-ubiquitylated proteins clustered to the autophagy pathway that were uniquely present in mutant cyclin F^{S621G}-expressing cells, and subsequently have verified specific dysfunction in autophagosomal formation and fusion in cells expressing cyclin F^{S621G}.

Lys48 ubiquitylation of proteins is elevated in mutant cyclin F^{S621G}-expressing cells

E3 ligases mediate the recognition of proteins targeted for degradation by covalently attaching mono- and poly-Lys48-ubiquitin chains to these proteins. Several studies have indicated that mutations, deficiency or dysfunction of ubiquitin E3 ligases, lead to neurodegenerative diseases [34–37]. To examine global polyubiquitylation differences between cells expressing cyclin F^{WT} and cyclin F^{S621G}, Neuro-2A cell lysates were immunoblotted for Lys48 ubiquitin and Lys63 ubiquitin. Lys48 ubiquitylation was approximately twofold higher (2.01-fold, $n = 3$, $p = 0.014$) in mutant cyclin F^{S621G}-expressing cells compared to wild-type controls (Fig. 1a), while there were no statistically significant differences observed in Lys63 ubiquitylation (1.19-fold, $n = 3$, $p = 0.0897$, Fig. 1b). We next verified the elevation of Lys48 ubiquitylation by immunofluorescence microscopy of Neuro-2A cells expressing mCherry-tagged cyclin F by quantifying the levels of Lys48 ubiquitylation in cells expressing mCherry alone (Fig. 1c). The degree of co-localization between mCherry-cyclin F and Lys48 ubiquitin was analysed using Mander's correlation coefficient. This revealed a significant increase (≥1.4-fold, $n = 19$, $p \leq 0.0001$) in the Lys48 ubiquitylation in cells expressing cyclin F^{S621G} compared to the cyclin F^{WT} control (Fig. 1c). Mutant cyclin F^{S621G}-expressing cells revealed a high ($R^2 = 0.89$) correlation between the level of Lys48 ubiquitylation and cyclin F-tagged mCherry, compared to cyclin F^{WT}-expressing cells ($R^2 = 0.67$). Collectively, these data indicate that expression of cyclin F^{S621G} contributes, either directly or indirectly, to the increased Lys48 ubiquitylation of cellular proteins in transfected Neuro-2A cells.

We have reported that ubiquitin-mediated proteasome degradation was impaired in NSC-34 cells transfected with mutant cyclin F^{S621G}, but proteasome function was unaffected in both wild type and mutant cyclin

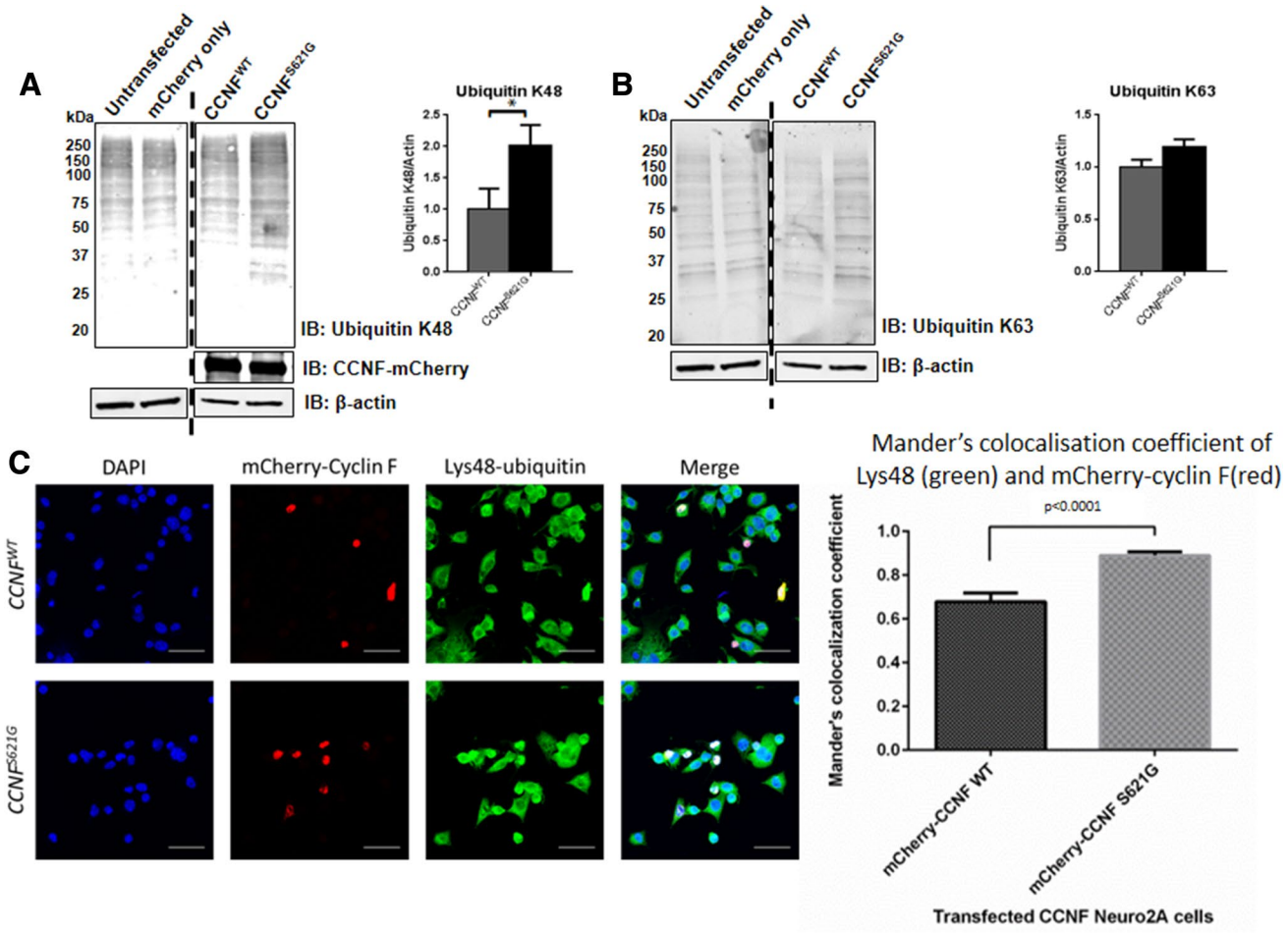

Fig. 1 Aberrant Lys48-specific ubiquitylation of proteins in mutant cyclin F^{S621G}-expressing Neuro-2A cells. **a** Immunoblot analyses of cyclin F^{WT} and mutant cyclin F^{S621G} cell lysates showed increased Lys48 ubiquitylation of cellular proteins in the mutant compared to the wild type (unpaired *t* test, $p = 0.014$, $n = 3$). *Vertical dashed line* indicates cropped lanes. **b** No statistically significant differences were observed in Lys63 ubiquitylation of cellular proteins between cyclin F^{WT} and mutant cyclin F^{S621G}-expressing Neuro-2A cells. **c** Immunofluorescence microscopy of transfected Neuro-2A cells demonstrated elevated Lys48-ubiquitylation in cells expressing mCherry-cyclin F^{S621G} relative to those expressing mCherry-cyclin F^{WT} by ~1.4-fold (unpaired two sample *t* test with Welch's correction, $p \leq 0.0001$, $n = 19$). Mander's co-localization coefficient measured the level of Lys48 ubiquitylation in only mCherry-expressing cells. *Scale bars* 50 µm

F^{S621G}-expressing cells, as they displayed relatively similar protein turnover rates [1]. Therefore, the higher levels of global Lys48 ubiquitylation of protein substrates in mutant cyclin F^{S621G}-expressing cells suggest either impairment to the enzymatic process and/or transportation of ubiquitylated substrates to the proteasome. Notably, no apparent differences were detected in bulk quantification of Lys63 ubiquitylation, demonstrating the specificity of mutant cyclin F^{S621G} upon Lys48-specific ubiquitylation. We examined the E3 ligase activity of wild type and mutant cyclin F^{S621G} by immunoprecipitating mCherry and performing E3 ligase assays on protein A/G beads using a commercial ELISA (Fig. 2). The E3 ligase activity of mutant cyclin F^{S621G} was approximately 1.35-fold higher than the wild type (Fig. 2), which is consistent with the increase in Lys48 ubiquitylation of cellular proteins observed by immunoblotting (Fig. 1a).

Different subsets of proteins are Lys48-ubiquitylated in cells expressing cyclin F^{WT} and cyclin F^{S621G}-transfected cells

Using Lys48-ubiquitin immunoprecipitations and LC–MS/MS, we employed a shotgun proteomics approach to determine the proteomic differences in Lys48-ubiquitylated proteins between cyclin F^{WT} and cyclin F^{S621G}-expressing cells. From triplicate analysis, 88 immunoprecipitated proteins were detected from cells expressing the mCherry-only construct and we considered these proteins to be constituents of the basal Lys48-ubiquitylated proteome. Of the three

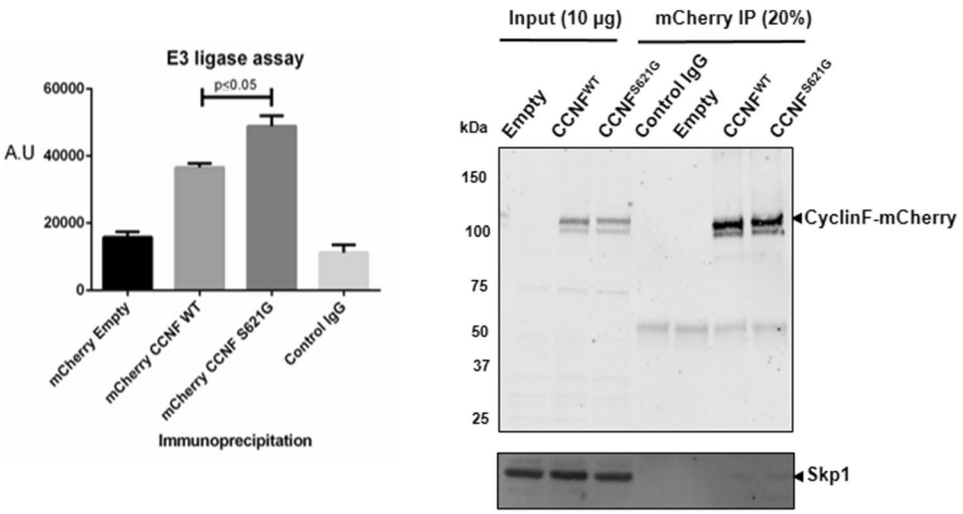

Fig. 2 E3 ligase activity of mutant cyclin F^{S621G} is elevated. E3 ligase activity of Lys48 ubiquitylation was elevated in Neuro-2A cells expressing mutant cyclin F^{S621G} compared to the $cyclin^{WT}$ control (Student *t* test, $p = 0.0228$, $n = 3$). Immunoblot analysis of the immunoprecipitant after the E3 ubiquitin reaction indicated equivalent enrichment of mCherry-cyclin F

transfected cell lines, 62 proteins were commonly enriched. In addition, we identified 395 and 205 immunoprecipitated proteins from cyclin F^{WT} and cyclin F^{S621G} cells, respectively (Fig. 3a). Although 92 proteins were common, different subsets of proteins were immunoprecipitated from cyclin F^{WT} (234 unique) and cyclin F^{S621G} (43 unique)-expressing cells (Fig. 3a; Supplementary Information). We validated a subset of the co-immunoprecipitated proteins by confirming the Lys48-ubiquitin status of selected proteins (p62/SQSTM1, profilin, and cyclin F) by immunoprecipitations followed by immunoblot analysis in cells expressing cyclin F^{WT} and mutant cyclin F^{S621G} (Fig. 3b).

Gene ontology analysis of the three subsets of Lys48-ubiquitylated proteins between transfected mCherry, cyclin F^{WT}, and cyclin F^{S621G} cells, revealed subtle differences in the types of proteins based on their molecular function (Supplementary Information), although no ontologies discriminated between the wild type and mutant. Therefore, we used Ingenuity Pathway Analysis (IPA) to determine whether Lys48-ubiquitylated proteins identified from cyclin F^{WT} and cyclin F^{S621G} cells clustered into specific biological networks and signaling pathways. Interestingly, there was a higher percentage of Lys48-ubiquitylated proteins found in mutant cyclin F^{S621G} cells that are involved in cellular maintenance and cytoskeletal organisation compared to the wild type (Fig. 3c). Specifically, these proteins clustered into functional IPA categories including Cell Death and Survival (such as ATG7 and CCT complexes), Cellular Assembly (such as NEFH and NEFL), Cell Function and Maintenance (such as CFL1 and APC), and Cellular Compromise (such as MAP1B and HSPA5) (Fig. 3c). Of these, only mutant cyclin F^{S621G} cells showed Lys48-ubiquitylated proteins clustered to specific protein networks such as the chaperonin (CCT) complexes that transport proteins to the autophagy machinery and various constituents of the autophagy pathway itself (Fig. 4) [38]. ATG7, HSP90, CTLA4, MAPT, RELN, CCT8, LRP5, and SHC1 were uniquely identified in the Lys48 immunoprecipitation from the mutant cyclin F^{S621G} cells. These findings provided a rationale to further investigate whether mutant cyclin F^{S621G} could disrupt the macroautophagy process within cyclin F-expressing cells.

Defective autophagy in SH-SY5Y cells expressing ALS/FTD-mutant cyclin F^{S621G}

For the autophagy degradation process to occur, cytoplasmic contents (including organelles) are first enclosed by a phagophore to form an autophagosome. Second, the outer membrane of the autophagosome fuses with the endosome, and subsequently the lysosome. Finally, once fusion is initiated, the contents of the autophagosome are released and subsequently degraded by lysosomal acidic hydrolases [39]. We assessed markers of macroautophagy by immunoblotting analysis of lysosome-associated membrane protein 2A (Lamp2A), LC3, and p62/SQSTM1, respectively (Fig. 5a). Interestingly, compared to cells transfected with the pcDNA3.1 vector, we observed increased levels of Lamp2A in cells expressing mutant cyclin F^{S621G} (1.35-fold, $n = 3$, $p = 0.0475$) and cyclin F^{WT} (1.54-fold, $n = 3$, $p = 0.0318$), suggesting a defect in fusion of the lysosome to the autophagosome during macroautophagy. Next, we immunoblotted for LC3, a marker of early phagophore formation, and identified that the level of LC3-II normalised to the GAPDH loading control [33] was decreased in cells expressing mutant cyclin F^{S621G} (0.75-fold, $n = 3$, $p = 0.0351$). This suggests decreased conversion of LC3-I–LC3-II, which is indicative of decreased formation of the autophagosome, and therefore, that fusion to the lysosome may be impaired in mutant cyclin F^{S621G}-expressing cells under normal conditions. Finally, we measured the levels of p62/SQSTM1, a marker of autophagy induction/flux, and found that p62/SQSTM1 was elevated in cells expressing mutant cyclin

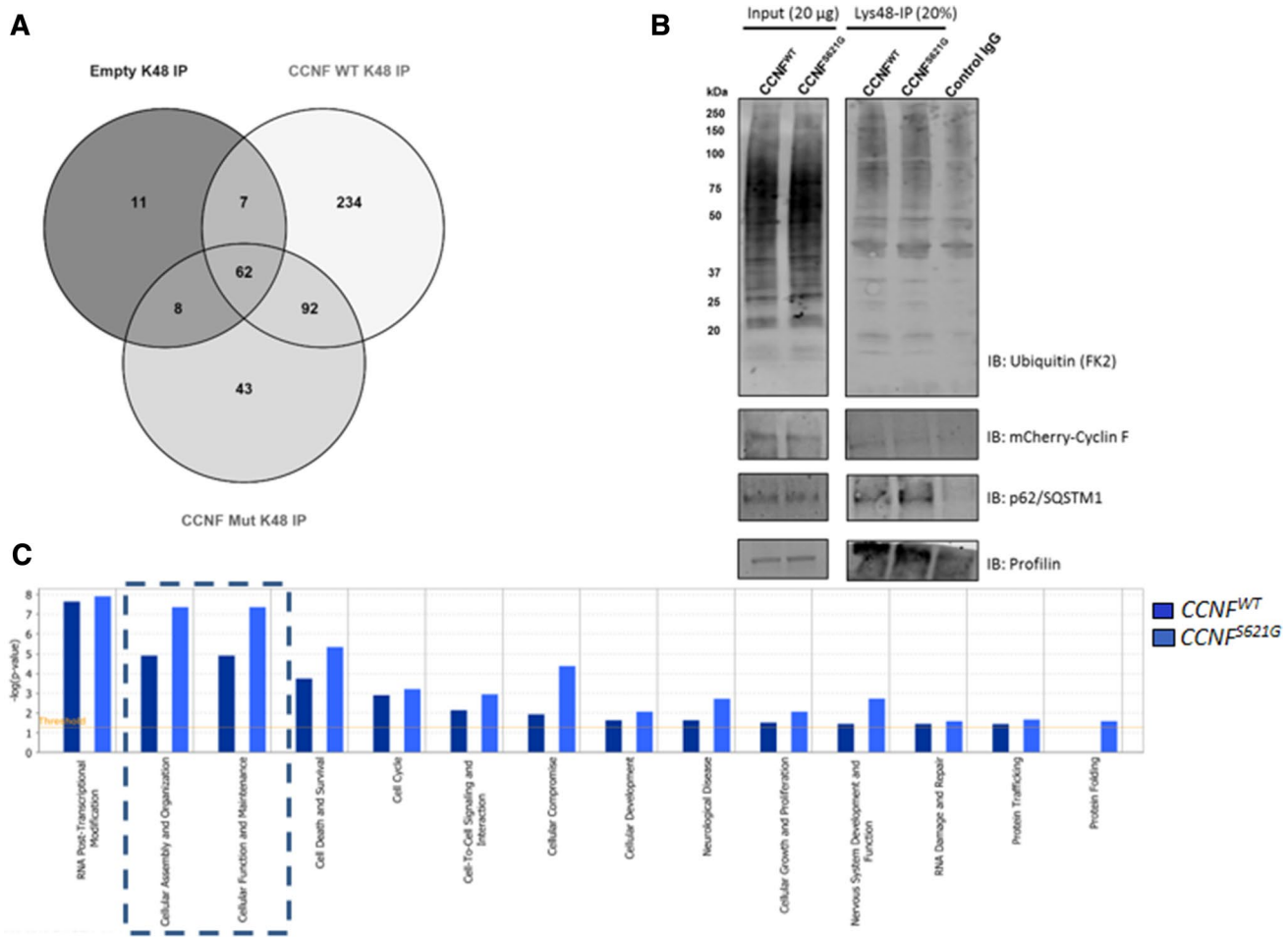

Fig. 3 Common and unique proteins identified from Lys48 immunoprecipitations. **a** Proteomic analysis of immunoprecipitated Lys48-ubiquitylated proteins from Neuro-2A cell lysates shows unique and common proteins between cells transfected with only mCherry, mCherry-cyclin $F^{WT,}$ and mutant mCherry-cyclin F^{S621G} ($n = 5$). **b)** Validation of proteomics analysis by Lys48-ubiquitin immunoprecipitations of mCherry-cyclin F^{WT} and mCherry-cyclin F^{S621G} cell lysates followed by immunoblots for ubiquitin, mCherry-cyclin F, p62/SQSTM1, and profilin ($n = 3$). **c** Ingenuity Pathway Analysis (IPA) revealed statistically significant differences in proteins clustered to biological processes involved in cellular assembly and organisation (Right tail Fischer Exact Test, cyclin F^{WT}, $p = 1.23 \times 10^{-5}$, cyclin F^{S621G}, $p = 4.37 \times 10^{-8}$), and cell death and survival (Right tail Fischer Exact Test, cyclin F^{WT}, $p = 1.79 \times 10^{-4}$, cyclin F^{S621G}, $p = 4.56 \times 10^{-6}$)

F^{S621G} (1.39-fold, $n = 3$, $p = 0.0486$) compared to the wild type. Increased p62/SQSTM1 levels have been used as a marker for inhibition of autophagy or defects to autophagic degradation [40–43], and is often used as a marker for autophagy induction [44, 45]. The increased levels of the adaptor protein p62/SQSTM1 in mutant cyclin F^{S621G} cells may indicate that either (1) substrates are being transported to the autophagosome but not degraded leading to an accumulation of p62/SQSTM1 and/or (2) both degradative pathways (autophagy and UPS) are unable to sustain the increased levels of Lys48-ubiquitylated substrates caused by hyper-ubiquitylation activity of mutant cyclin F. In this manner, mutant cyclin F^{S621G} creates a circular cascade that leads to progressive accumulation of Lys48-ubiquitylated proteins. Supporting our findings, Korolchuk and colleagues demonstrated that dysfunctional macroautophagy resulted in p62/SQSTM1 accumulation and consequently led to increased levels of ubiquitylated proteins that compromised their delivery and degradation by the UPS [46].

To verify whether the increased levels of Lys48-ubiquitylated proteins was due to decreased level of protein degradation or defects in the autophagy pathway, we examined the fusion of autophagosomes to lysosomes by expression of a tandem mCherry-EGFP-LC3 construct [33, 47], using serum starvation to induce autophagy (Fig. 5b). This assay is based on the nature of the GFP protein, which is highly sensitive to the acidic environment of the lysosomes. Under these conditions, the signal from GFP is quenched within

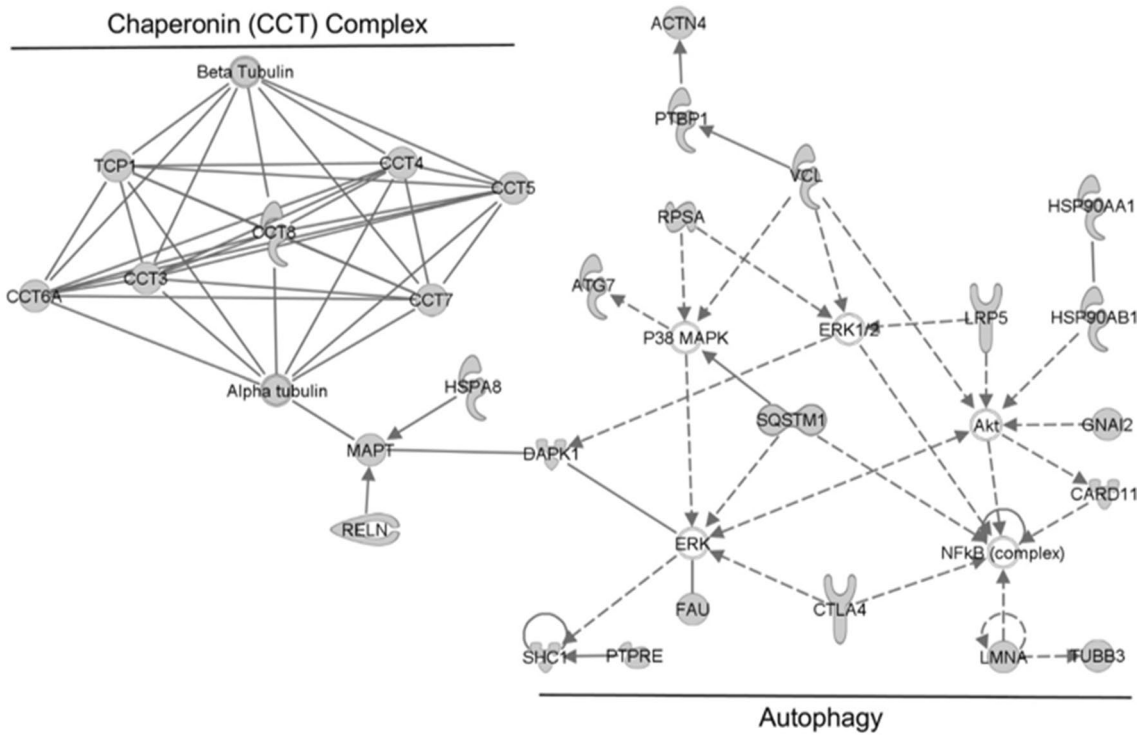

Fig. 4 Lys48-ubiquitylated proteins identified in cells expressing mutant cyclin F^{S621G} clustered to the autophagy pathway. Proteomics analysis of Lys48 immunoprecipitates from Neuro-2A cells expressing only mutant cyclin F^{S621G} identified components of the molecular chaperone machinery and autophagy pathway. *Bolded* and *dashed lines* indicate direct and indirect interactions, respectively, and components coloured in *grey* identified by LC–MS/MS. ATG7, HSP90, CTLA4, MAPT, RELN, CCT8, LRP5, and SHC1 were uniquely identified in the Lys48 immunoprecipitation from the mutant cyclin F^{S621G} cells

the lysosome, whereas mCherry is stable. Thus, in the non-acidic environment of autophagosomes, before fusion with lysosomes, LC3 puncta show both GFP and mCherry signals, but once the maturation to autophagolysosomes occurs, only the mCherry signal will be present [47]. The fusion of the autophagosome to the lysosome is thought to cause displacement of its contents within the acidic environment of the lysosome for degradation. That is, the presence of co-localization of both mCherry and GFP fluorescence is indicative of improper fusion of the autophagosome to the lysosome, whereas observations of mCherry fluorescence alone correspond to proper fusion, mature autophagolysosome formation, and suggests downstream clearance of substrates [33].

SH-SY5Y cells were either untransfected or transfected with pcDNA3.1, FLAG-$CCNF^{WT}$, or FLAG-$CCNF^{S621G}$ for 48 h. Following transfections and serum starvation to induce autophagy, we observed no statistical difference in autophagosome and lysosomes between untransfected and pcDNA3.1 controls, with both showing quenching of the GFP signal indicative of proper fusion to the lysosome (Fig. 5b, c). Elevated levels of autophagosomes were observed in cells expressing mCherry-EGFP-LC3 and FLAG-cyclin F^{S621G} compared to cells expressing pcDNA3.1 (1.96-fold, $p \leq 0.0001$) and FLAG-cyclin F^{WT} (1.68-fold, $p \leq 0.0001$) (Fig. 5c). Accordingly, the levels of autolysosomes were reduced in cells expressing mutant FLAG-cyclin F^{S621G} compared to pcDNA3.1 (0.51-fold, $p \leq 0.0001$) and FLAG-cyclin F^{WT} (0.59-fold, $p \leq 0.0001$), suggesting that the fusion of the autophagosome to the lysosome is impaired in mutant cyclin F^{S621G}-expressing cells, thus possibly affecting the degradation and clearance of substrates.

Defective autophagy recapitulated in HEK293 and human primary fibroblast cells expressing mutant cyclin F^{S621G}

To confirm whether cyclin F^{S621G} overexpression causes defects in the autophagy pathway in other cell types, we repeated these experiments in transiently transfected HEK293 cells and human primary fibroblasts derived from an ALS patient with the $CCNF^{S621G}$ mutation. In HEK293 cells, we observed similar results to the experiments carried out in SH-SY5Y cells (Fig. 5a). Specifically, immunoblot analyses revealed increased expression of p62/SQSTM1 by 1.41-fold (unpaired *t* test, $n = 3$, $p = 0.0476$) and reduced LC3-I–LC3-II conversion by 0.78-fold (unpaired *t* test,

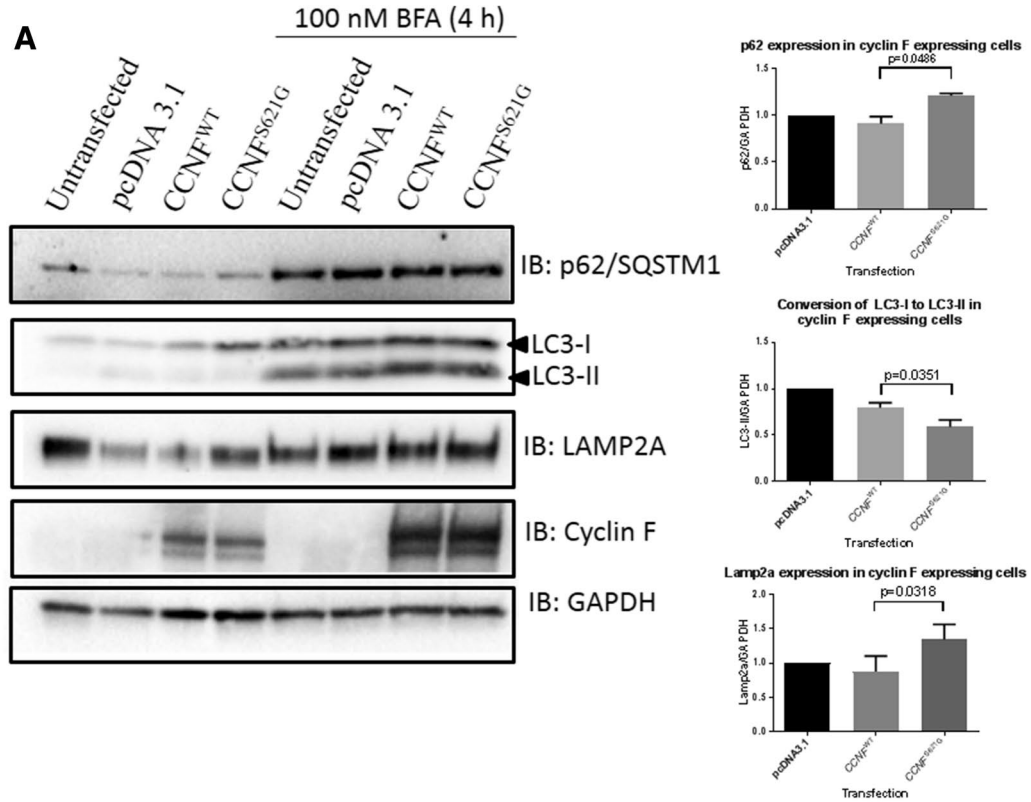
A
100 nM BFA (4 h)
Untransfected
pcDNA 3.1
CCNF^WT
CCNF^S621G
Untransfected
pcDNA 3.1
CCNF^WT
CCNF^S621G
IB: p62/SQSTM1
LC3-I
LC3-II
IB: LAMP2A
IB: Cyclin F
IB: GAPDH
p62 expression in cyclin F expressing cells
p=0.0486
p62/GA PDH
Transfection
Conversion of LC3-I to LC3-II in cyclin F expressing cells
p=0.0351
LC3-II/GA PDH
Transfection
Lamp2a expression in cyclin F expressing cells
p=0.0318
Lamp2a/GA PDH
Transfection

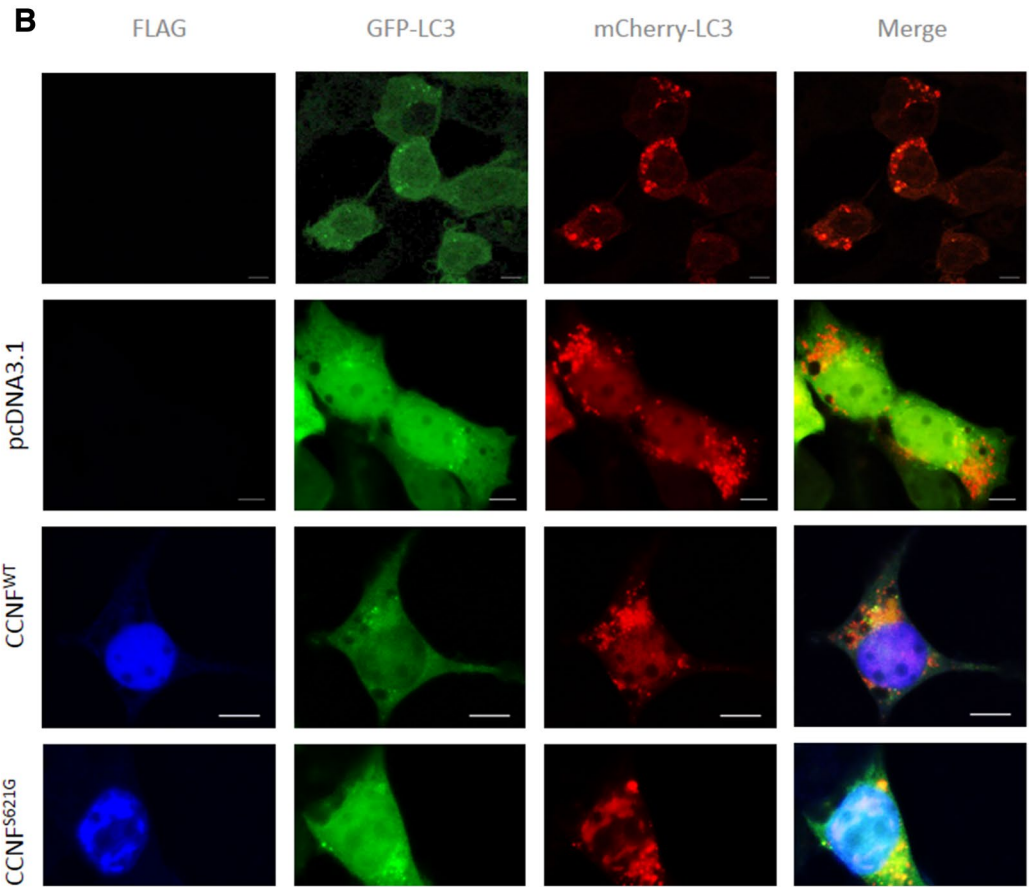
B
FLAG
GFP-LC3
mCherry-LC3
Merge
pcDNA3.1
CCNF^WT
CCNF^S621G

◀ **Fig. 5** Impaired autophagosomal fusion and formation in SH-SY5Y cells expressing cyclin F^{S621G}. **a** Immunoblot analyses of autophagy markers LC3, p62/SQSTM1, Lamp2a in untransfected, mCherry-only, mCherry-cyclin F^{WT} and mCherry-cyclin F^{S621G}-expressing cells shows the reduced conversion of LC3-I to LC3-II by 0.75-fold (unpaired *t* test, $n = 3$, $p = 0.0351$) and 0.31-fold (unpaired *t* test, $n = 3$, $p = 0.0048$) under normal and bafilomycin (100 nM, 4 h) conditions, respectively, in mutant cyclin F^{S621G} cells compared to the wild type. Increased expression of p62/SQSTM1 by 1.32-fold (unpaired *t* test, $n = 3$, $p = 0.0486$) and Lamp2a by 1.55-fold (unpaired *t* test, $n = 3$, $p = 0.0318$) was observed in mutant cyclin F^{S621G} cells compared to the wild type. Densitometry values were normalised to GAPDH and subsequently to the pcDNA3.1 controls. **b** SH-SY5Y cells expressing pCDNA3.1, FLAG-cyclin F^{WT}, FLAG-cyclin F^{S621G}, and mCherry-GFP-LC3 were serum-starved for 6 h to induce autophagy. The fluorescence of GFP was measured from the fusion protein, and there was decreased proportion of mCherry-positive mature autolysosomes due to the reduced quenching of the green fluorescence, indicating that fusion between autophagosomes and lysosomes is impaired in mutant cyclin F^{S621G} cells. *Scale bars* 10 µm. **c** Quantification of the percentage of vesicles with mCherry-GFP-LC3 only positive autolysosomes relative to total puncta per cell in at least 25 cells from each sample, $n = 3$. Data are represented as the mean ± SEM; $^{****}p < 0.0001$ using one-way ANOVA with Tukey's post hoc test

$n = 3$, $p = 0.0136$) in mutant cyclin F^{S621G} cells compared to the wild-type-expressing cells under normal conditions, thus recapitulating the previous observations (Fig. 6a).

As described previously, in accordance with the new international guidelines for the experimental measurement of autophagy function by Klionsky et al., transfected HEK293 cells were treated with bafilomycin to inhibit the fusion of autophagosomes to the lysosome, which resulted in a further reduction (by 0.31-fold, $n = 3$, $p = 0.0048$) in LC3-I-to-LC3-II conversion in mutant cyclin F^{S621G} cells compared to the wild-type cells. It would be expected that by blocking mature autophagosome fusion to the lysosome with bafilomycin, an accumulation of LC3-II would occur. This was observed to a lesser extent in the mutant cyclin F^{S621G} cells compared to the untransfected, pcDNA3.1, and wild-type cyclin F-transfected cells. This would suggest that the formation of mature autophagosomes is impaired in mutant cyclin F^{S621G} cells, resulting in reduced fusion to the lysosome (as observed in Fig. 5c) and possibly downstream clearance of substrates through the autophagy pathway. These findings further indicate that defects to the observed autophagy pathway were indeed due to the effects of the cyclin F^{S621G} mutation and not as a consequence of the transfection protocol, which specifically demonstrate impairments to the formation of mature autophagosomes.

We next examined by immunoblotting analysis human primary fibroblast cultures from non-disease control, non-disease *CCNF*^{S621G} carrier, and ALS–affected *CCNF*^{S621G} patients that were cultured in technical triplicates. In accordance with observations from SH-SY5Y and HEK293 cells, expression of p62/SQSTM1 was increased by 1.57-fold in both the non-disease carrier (one-way ANOVA, $n = 3$, $p = 0.0267$) and 1.39-fold in the ALS patient fibroblasts (one-way ANOVA, $n = 3$, $p = 0.0146$) compared to fibroblasts from non-disease control patients (Fig. 6b). Surprisingly, however, immunoblotting analysis revealed increased LC3-II by 4.23-fold (carrier) (one-way ANOVA, $n = 3$, $p \leq 0.0001$) and 3.17-fold (affected) (one-way ANOVA *t* test, $n = 3$, $p \leq 0.0001$) compared to the non-disease control (Fig. 6b). While this is the opposite response to that observed in transiently transfected cell lines, this might reflect the fact that the patient fibroblasts constitutively express cyclin F^{S621G} and have been maintained in culture

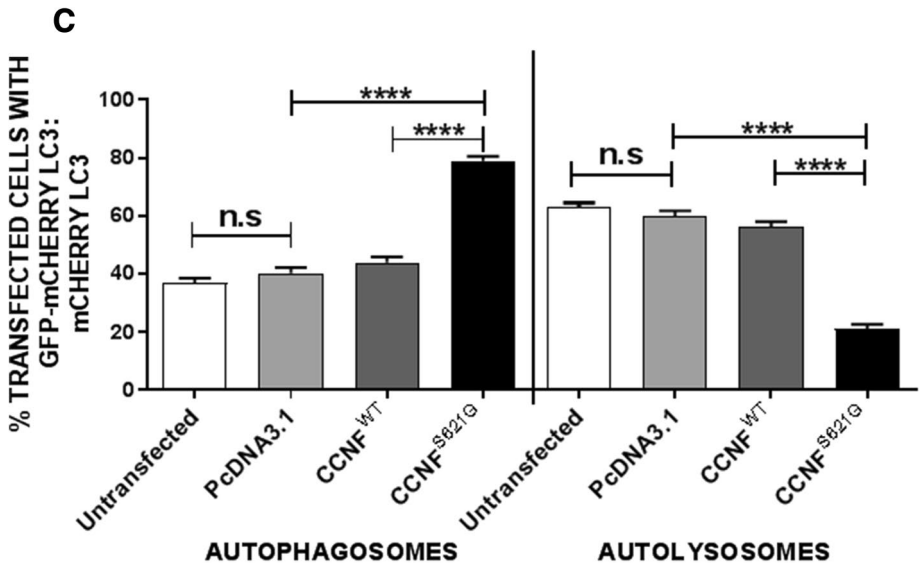

Fig. 5 (continued)

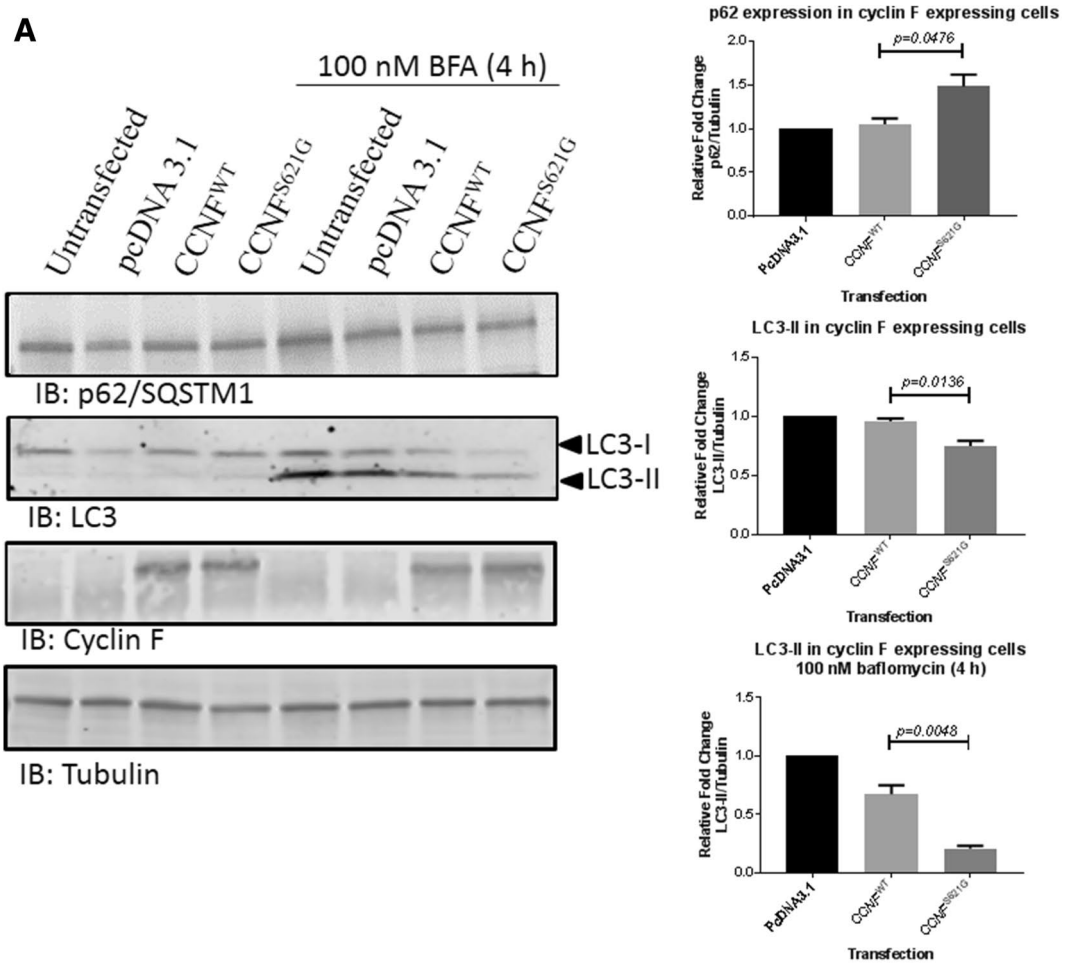
A
100 nM BFA (4 h)
Untransfected
pcDNA 3.1
CCNF^WT
CCNF^S621G
Untransfected
pcDNA 3.1
CCNF^WT
CCNF^S621G
IB: p62/SQSTM1
LC3-I
LC3-II
IB: LC3
IB: Cyclin F
IB: Tubulin
p62 expression in cyclin F expressing cells
p=0.0476
Relative Fold Change p62/Tubulin
PcDNA3.1
CCNF^WT
CCNF^S621G
Transfection
LC3-II in cyclin F expressing cells
p=0.0136
Relative Fold Change LC3-II/Tubulin
Transfection
LC3-II in cyclin F expressing cells
100 nM baflomycin (4 h)
p=0.0048
Relative Fold Change LC3-II/Tubulin
Transfection

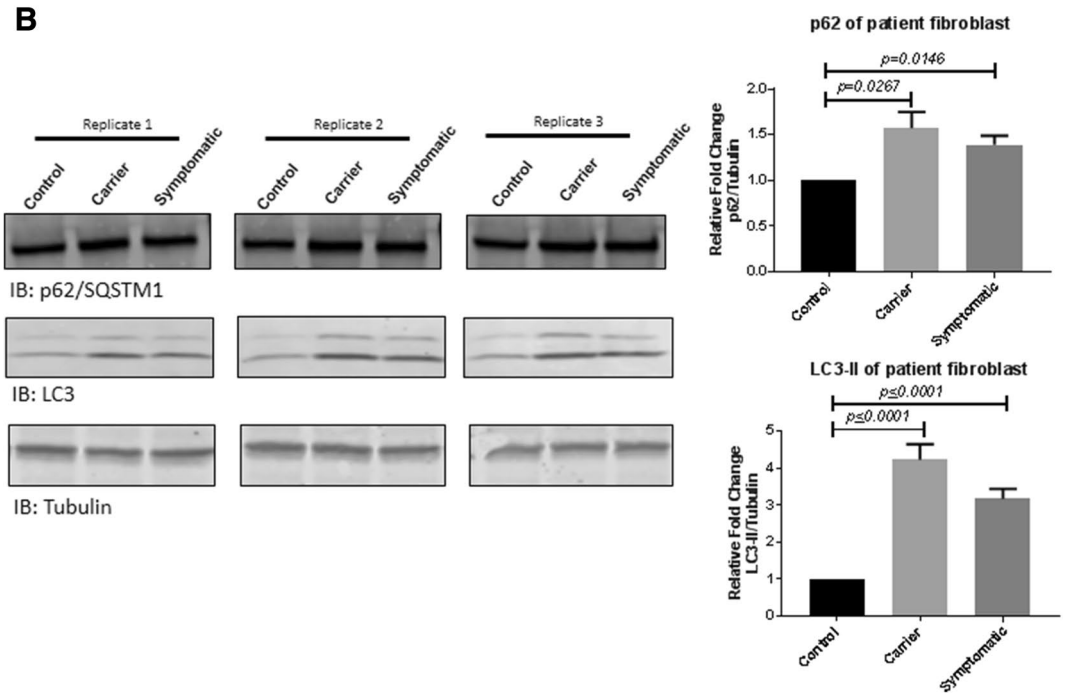
B
Replicate 1
Replicate 2
Replicate 3
Control
Carrier
Symptomatic
IB: p62/SQSTM1
IB: LC3
IB: Tubulin
p62 of patient fibroblast
p=0.0146
p=0.0267
Relative Fold Change p62/Tubulin
LC3-II of patient fibroblast
p≤0.0001
p≤0.0001
Relative Fold Change LC3-II/Tubulin

◂**Fig. 6** Impaired autophagy recapitulated in HEK293 cells expressing cyclin F^{S621G} cells and increased p62 and LC3-II levels in patient fibroblasts. **a** Immunoblot analyses of autophagy markers LC3, p62/SQSTM1, Lamp2a in untransfected, pcDNA3.1 only, FLAG-cyclin F^{WT}, and FLAG-cyclin F^{S621G}-expressing cells shows the reduced conversion of LC3-I–LC3-II by 0.78-fold (unpaired *t* test, $n = 3$, $p = 0.0136$) and increased expression of p62/SQSTM1 by 1.41-fold (unpaired *t* test, $n = 3$, $p = 0.0476$) in mutant cyclin F^{S621G}-expressing cells. Densitometry values were normalised to tubulin and subsequently to the pcDNA3.1 controls. **b** Primary fibroblast cultures (non-disease control, $CCNF^{S621G}$ carrier, and $CCNF^{S621G}$ affected patient) were grown in triplicate, and immunoblot analysis revealed increased p62/SQSTM1 by 1.57-fold (carrier) (one-way ANOVA Dunnett's multiple comparison test, $n = 3$, $p = 0.0267$) and 1.39-fold (affected) (one-way ANOVA Dunnett's multiple comparison test, $n = 3$, $p = 0.0146$) compared to the non-disease control patients. Immunoblot analysis also revealed increased conversion of LC3-I–LC3-II by 4.23-fold (carrier) (one-way ANOVA Dunnett's multiple comparison test, $n = 3$, $p \leq 0.0001$) and 3.17-fold (affected) (one-way ANOVA Dunnett's multiple comparison test, $n = 3$, $p \leq 0.0001$) compared to the non-disease control

for several months, as compared to cell lines which have been maintained for approximately 1 week. Furthermore, the increased LC3-I-to-LC3-II conversion in $CCNF^{S621G}$ carriers is consistent with autophagosome accumulation as observed in SH-SY5Y cells (Fig. 5b, c), which, therefore, confirms that expression of cyclin F^{S621G} causes autophagic defects in patient fibroblasts. We were unable to perform bafilomycin treatment controls with the primary fibroblasts because of poor cell viability in the presence of bafilomycin, which we presume is due to the sensitive nature of primary cells in culture.

Increased p62/SQSTM1 ubiquitylation in cells expressing mutant cyclin F^{S621G}

One possible scenario by which neuronal-like cells expressing mutant cyclin F might cause impairments to autophagosome formation and fusion could be that elevated E3 ligase activity of mutant cyclin F may alter cellular ubiquitin homeostasis ("Ubiquitin Stress") [48]. Under ubiquitin stress, the receptor p62/SQSTM1 is ubiquitylated, which disrupts its dimerization, liberating its ability to recognise polyubiquitylated cargoes for selective autophagy [48]. P62/SQSTM1 is localised to ubiquitin-positive inclusions and critical for the aggregation of ubiquitylated proteins, which are commonly observed in neurodegenerative diseases [41, 49, 50].

We demonstrated that p62/SQSTM1 was indeed Lys48-ubiquitylated in both cells expressing wild type and mutant cyclin F^{S621G} (Fig. 3b), and increased levels of p62 were evident in SH-SY5Y (Fig. 5a), HEK293 (Fig. 6a), and primary fibroblast cultures from cyclin F^{S621G} patients (Fig. 6b). Therefore, to determine the ubiquitylation status of p62/SQSTM1 in HEK293 cells transfected with wild type and mutant cyclin F^{S621G}, we immunoprecipitated p62/SQSTM1 from untransfected, pcDNA3.1, FLAG-cyclin F^{WT}, and FLAG-cyclin F^{S621G}-expressing cells, and immunoblotted for ubiquitin and cyclin F. Intriguingly, we determined that p62/SQSTM1 was more ubiquitylated in the mutant cyclin F^{S621G} cells by approximately 2.22-fold ($n = 5$, $p \leq 0.0001$) compared to the wild-type controls. We also determined increased co-interaction of immunoprecipitated p62/SQSTM1 with mutant cyclin F^{S621G} by approximately 1.2-fold compared to the FLAG-cyclin F^{WT} ($n = 5$, $p \leq 0.0001$) (Fig. 7). These results suggest that one possible mechanism by which mutant cyclin F^{S621G} may cause impairments to the autophagy pathway could be through direct binding and increased ubiquitylation of the p62/SQSTM1 receptor that controls the transport of ubiquitylated substrates for autophagic degradation.

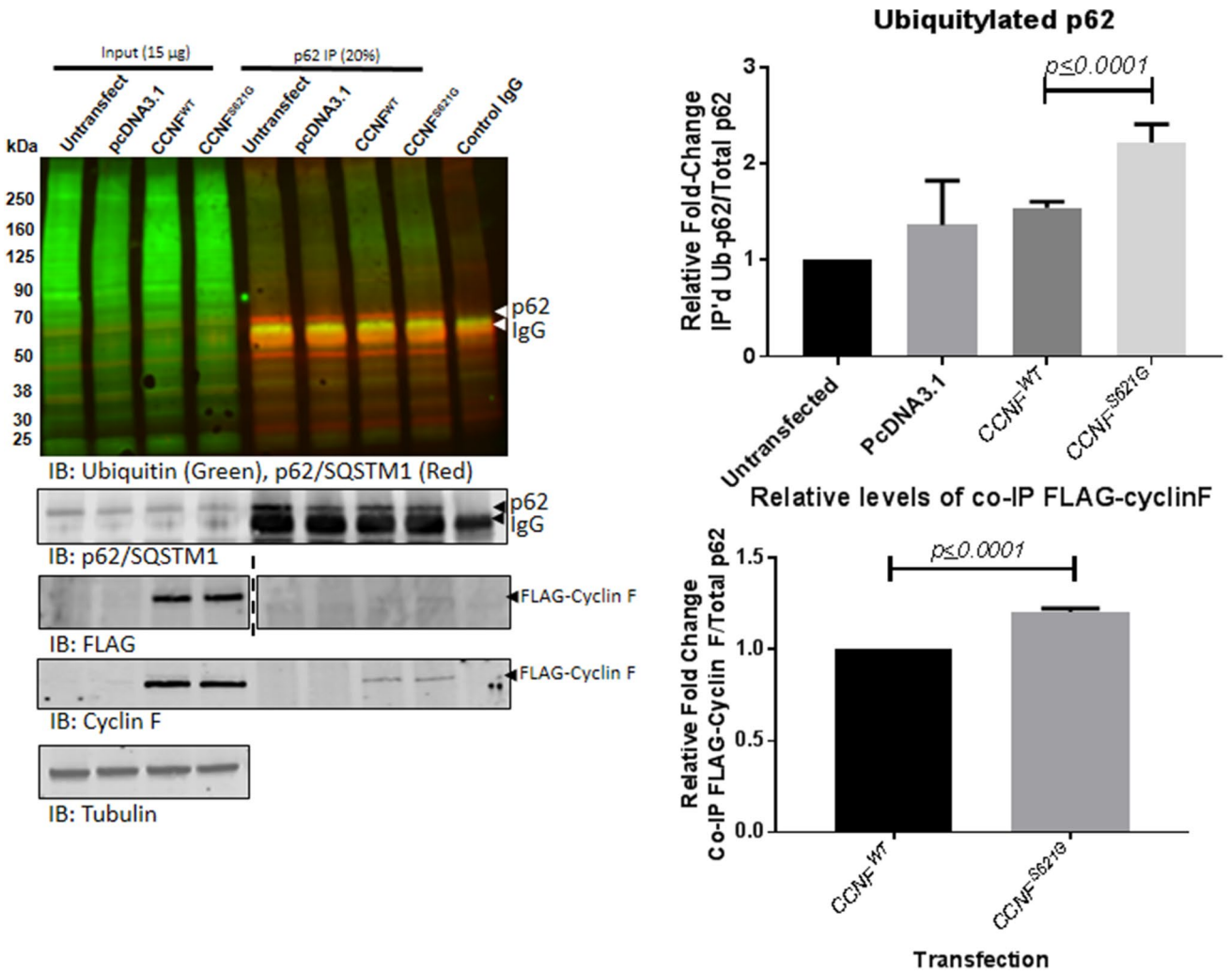

Fig. 7 Increased ubiquitylation of p62 and co-interaction to mutant cyclin F^{S621G}. Neuro-2A cells were transfected with pcDNA 3.1, FLAG-*CCNF*^{WT}, and FLAG-*CCNF*^{S621G} for 24 h. p62/SQSTM1 was immunoprecipitated from cell lysates and immunoblotted for ubiquitin (*green*) and p62/SQSTM (*red*) and revealed increased ubiquitylation of p62/SQSTM1 in mutant cyclin F cells relative to the wild-type by approximately 1.44-fold (unpaired *t* test, $n = 5$, $p \leq 0.0001$). Immunoblot analysis of the p62/SQSTM1 immunoprecipitates with FLAG and cyclin F demonstrated increased co-interaction of mutant cyclin F^{S621G} by approximately 1.2-fold compared to cyclin F^{WT} (unpaired *t* test, $n = 5$, $p \leq 0.0001$). The relative levels of ubiquitylated p62 and co-immunoprecipitated cyclin F were normalised to the total levels of immunoprecipitated p62, and subsequently normalised to either p62 levels in the untransfected or cyclin F^{WT}-expressing cells. *Vertical dashed line* indicate cropped lanes

Conclusion

In summary, we have identified increased Lys48 ubiquitylation of cellular proteins in mutant cyclin F^{S621G}-expressing neuronal-like cells as a consequence of elevated E3 ligase activity of mutant cyclin F. The Lys48-ubiquitylated proteome differed amongst cells expressing wild type and mutant cyclin F^{S621G}, with various components of the chaperonin complex and autophagy pathway identified in mutant cyclin F^{S621G}-expressing cells. We verified alterations in the levels of markers of autophagy (Lamp2a, LC3, and p62/SQSTM1) by immunoblotting and immunofluorescence microscopy that indicate impairment to autophagosome formation and fusion in cell lines transiently expressing mutant cyclin F^{S621G} and in patient fibroblasts bearing the pathogenic cyclin F^{S621G}. This suggests that abnormal ubiquitylation activity of cyclin F (caused by mutation or other deficiency) leads to functional impairment in the autophagy degradation pathway, which might represent an underlying molecular mechanism contributing to the pathogenesis of ALS/FTD.

Acknowledgements This research was supported by funding from the Motor Neurone Disease Research Institute of Australia (MNDRIA) (GIA1510, GIA1628, and GIA1715); MND Australia and National Health and Medical Research Council of Australia (NHMRC) Grants: APP1107644, APP1030513 and APP1095215, and NHMRC early

career fellowship APP1036835. This research was supported by access to the Australian Proteomics Analysis Facility (APAF) established under the Australian Government's NCRIS program. The authors acknowledge the support of the Macquarie University Centre for Motor Neuron Disease Research.

References

1. Williams KL, Topp S, Yang S, Smith B, Fifita JA, Warraich ST, Zhang KY, Farrawell N, Vance C, Hu X, Chesi A, Leblond CS, Lee A, Rayner SL, Sundaramoorthy V, Dobson-Stone C, Molloy MP, van Blitterswijk M, Dickson DW, Petersen RC, Graff-Radford NR, Boeve BF, Murray ME, Pottier C, Don E, Winnick C, McCann EP, Hogan A, Daoud H, Levert A, Dion PA, Mitsui J, Ishiura H, Takahashi Y, Goto J, Kost J, Gellera C, Gkazi AS, Miller J, Stockton J, Brooks WS, Boundy K, Polak M, Munoz-Blanco JL, Esteban-Perez J, Rabano A, Hardiman O, Morrison KE, Ticozzi N, Silani V, de Belleroche J, Glass JD, Kwok JB, Guillemin GJ, Chung RS, Tsuji S, Brown RH Jr., Garcia-Redondo A, Rademakers R, Landers JE, Gitler AD, Rouleau GA, Cole NJ, Yerbury JJ, Atkin JD, Shaw CE, Nicholson GA, Blair IP (2016) CCNF mutations in amyotrophic lateral sclerosis and frontotemporal dementia. Nat Commun 7:11253. doi:10.1038/ncomms11253
2. Hogan AL, Don EK, Rayner SL, Lee A, Laird AS, Watchon M, Winnick C, Tarr IS, Morsch M, Fifita JA, Gwee S, Formella I, Hortle E, Yuan K, Molloy MP, Williams KL, Nicholson GA, Chung RS, Blair IP, Cole NJ (2017) Expression of ALS/FTD-linked mutant CCNF in zebrafish leads to increased cell death in the spinal cord and an aberrant motor phenotype. Hum Mol Genet. doi:10.1093/hmg/ddx136
3. Bai C, Sen P, Hofmann K, Ma L, Goebl M, Harper JW, Elledge SJ (1996) SKP1 connects cell cycle regulators to the ubiquitin proteolysis machinery through a novel motif, the F-box. Cell 86(2):263–274
4. Ravid T, Hochstrasser M (2008) Diversity of degradation signals in the ubiquitin-proteasome system. Nat Rev Mol Cell Biol 9(9):679–690. doi:10.1038/nrm2468
5. Ikeda F, Dikic I (2008) Atypical ubiquitin chains: new molecular signals. 'Protein modifications: beyond the usual suspects' review series. EMBO Rep 9(6):536–542. doi:10.1038/embor.2008.93
6. Matsumoto G, Wada K, Okuno M, Kurosawa M, Nukina N (2011) Serine 403 phosphorylation of p62/SQSTM1 regulates selective autophagic clearance of ubiquitinated proteins. Mol Cell 44(2):279–289. doi:10.1016/j.molcel.2011.07.039
7. Wooten MW, Geetha T, Babu JR, Seibenhener ML, Peng J, Cox N, Diaz-Meco MT, Moscat J (2008) Essential role of sequestosome 1/p62 in regulating accumulation of Lys63-ubiquitinated proteins. J Biol Chem 283(11):6783–6789. doi:10.1074/jbc.M709496200
8. Lippai M, Low P (2014) The role of the selective adaptor p62 and ubiquitin-like proteins in autophagy. Biomed Res Int 2014:832704. doi:10.1155/2014/832704
9. Kirkin V, McEwan DG, Novak I, Dikic I (2009) A role for ubiquitin in selective autophagy. Mol Cell 34(3):259–269. doi:10.1016/j.molcel.2009.04.026
10. Long J, Gallagher TR, Cavey JR, Sheppard PW, Ralston SH, Layfield R, Searle MS (2008) Ubiquitin recognition by the ubiquitin-associated domain of p62 involves a novel conformational switch. J Biol Chem 283(9):5427–5440. doi:10.1074/jbc.M704973200
11. Jacobson AD, Zhang NY, Xu P, Han KJ, Noone S, Peng J, Liu CW (2009) The lysine 48 and lysine 63 ubiquitin conjugates are processed differently by the 26s proteasome. J Biol Chem 284(51):35485–35494. doi:10.1074/jbc.M109.052928
12. Nassif M, Valenzuela V, Rojas-Rivera D, Vidal R, Matus S, Castillo K, Fuentealba Y, Kroemer G, Levine B, Hetz C (2014) Pathogenic role of BECN1/Beclin 1 in the development of amyotrophic lateral sclerosis. Autophagy 10(7):1256–1271. doi:10.4161/auto.28784
13. Lattante S, de Calbiac H, Le Ber I, Brice A, Ciura S, Kabashi E (2015) Sqstm1 knock-down causes a locomotor phenotype ameliorated by rapamycin in a zebrafish model of ALS/FTLD. Hum Mol Genet 24(6):1682–1690. doi:10.1093/hmg/ddu580
14. Soo KY, Atkin JD (2015) Autophagy dysregulation by mutant fused in sarcoma–implications for amyotrophic lateral sclerosis. Cell Death Dis 6:e1945. doi:10.1038/cddis.2015.311
15. Soo KY, Sultana J, King AE, Atkinson R, Warraich ST, Sundaramoorthy V, Blair I, Farg MA, Atkin JD (2015) ALS-associated mutant FUS inhibits macroautophagy which is restored by overexpression of Rab1. Cell Death Discov 1:15030. doi:10.1038/cddiscovery.2015.30
16. Wang IF, Tsai KJ, Shen CK (2013) Autophagy activation ameliorates neuronal pathogenesis of FTLD-U mice: a new light for treatment of TARDBP/TDP-43 proteinopathies. Autophagy 9(2):239–240. doi:10.4161/auto.22526
17. Munch C, Sedlmeier R, Meyer T, Homberg V, Sperfeld AD, Kurt A, Prudlo J, Peraus G, Hanemann CO, Stumm G, Ludolph AC (2004) Point mutations of the p150 subunit of dynactin (DCTN1) gene in ALS. Neurology 63(4):724–726
18. Puls I, Jonnakuty C, LaMonte BH, Holzbaur EL, Tokito M, Mann E, Floeter MK, Bidus K, Drayna D, Oh SJ, Brown RH Jr., Ludlow CL, Fischbeck KH (2003) Mutant dynactin in motor neuron disease. Nat Genet 33(4):455–456. doi:10.1038/ng1123
19. Johnson JO, Mandrioli J, Benatar M, Abramzon Y, Van Deerlin VM, Trojanowski JQ, Gibbs JR, Brunetti M, Gronka S, Wuu J, Ding J, McCluskey L, Martinez-Lage M, Falcone D, Hernandez DG, Arepalli S, Chong S, Schymick JC, Rothstein J, Landi F, Wang YD, Calvo A, Mora G, Sabatelli M, Monsurro, Battistini S, Salvi F, Spataro R, Sola P, Borghero G, Consortium I, Galassi G, Scholz SW, Taylor JP, Restagno G, Chio A, Traynor BJ (2010) Exome sequencing reveals VCP mutations as a cause of familial ALS. Neuron 68(5):857–864. doi:10.1016/j.neuron.2010.11.036
20. Pilli M, Arko-Mensah J, Ponpuak M, Roberts E, Master S, Mandell MA, Dupont N, Ornatowski W, Jiang S, Bradfute SB, Bruun JA, Hansen TE, Johansen T, Deretic V (2012) TBK-1 promotes autophagy-mediated antimicrobial defense by controlling autophagosome maturation. Immunity 37(2):223–234. doi:10.1016/j.immuni.2012.04.015
21. Freischmidt A, Wieland T, Richter B, Ruf W, Schaeffer V, Muller K, Marroquin N, Nordin F, Hubers A, Weydt P, Pinto S, Press R, Millecamps S, Molko N, Bernard E, Desnuelle C, Soriani MH, Dorst J, Graf E, Nordstrom U, Feiler MS, Putz S, Boeckers TM, Meyer T, Winkler AS, Winkelman J, de Carvalho M, Thal DR, Otto M, Brannstrom T, Volk AE, Kursula P, Danzer KM, Lichtner P, Dikic I, Meitinger T, Ludolph AC, Strom TM, Andersen PM, Weishaupt JH (2015) Haploinsufficiency of TBK1 causes familial ALS and fronto-temporal dementia. Nat Neurosci 18(5):631–636. doi:10.1038/nn.4000
22. Shen WC, Li HY, Chen GC, Chern Y, Tu PH (2015) Mutations in the ubiquitin-binding domain of OPTN/optineurin interfere with autophagy-mediated degradation of misfolded proteins by a dominant-negative mechanism. Autophagy 11(4):685–700. doi:10.4161/auto.36098
23. Maruyama H, Morino H, Ito H, Izumi Y, Kato H, Watanabe Y, Kinoshita Y, Kamada M, Nodera H, Suzuki H, Komure O, Matsuura S, Kobatake K, Morimoto N, Abe K, Suzuki N, Aoki M, Kawata A, Hirai T, Kato T, Ogasawara K, Hirano A, Takumi T, Kusaka H, Hagiwara K, Kaji R, Kawakami H (2010) Mutations of optineurin in amyotrophic lateral sclerosis. Nature 465(7295):223–226. doi:10.1038/nature08971

24. Sundaramoorthy V, Walker AK, Tan V, Fifita JA, McCann EP, Williams KL, Blair IP, Guillemin GJ, Farg MA, Atkin JD (2015) Defects in optineurin- and myosin VI-mediated cellular trafficking in amyotrophic lateral sclerosis. Hum Mol Genet 24(13):3830–3846. doi:10.1093/hmg/ddv126
25. Cox LE, Ferraiuolo L, Goodall EF, Heath PR, Higginbottom A, Mortiboys H, Hollinger HC, Hartley JA, Brockington A, Burness CE, Morrison KE, Wharton SB, Grierson AJ, Ince PG, Kirby J, Shaw PJ (2010) Mutations in CHMP2B in lower motor neuron predominant amyotrophic lateral sclerosis (ALS). PLoS One 5(3):e9872. doi:10.1371/journal.pone.0009872
26. Komatsu M, Waguri S, Chiba T, Murata S, Iwata J, Tanida I, Ueno T, Koike M, Uchiyama Y, Kominami E, Tanaka K (2006) Loss of autophagy in the central nervous system causes neurodegeneration in mice. Nature 441(7095):880–884. doi:10.1038/nature04723
27. Hara T, Nakamura K, Matsui M, Yamamoto A, Nakahara Y, Suzuki-Migishima R, Yokoyama M, Mishima K, Saito I, Okano H, Mizushima N (2006) Suppression of basal autophagy in neural cells causes neurodegenerative disease in mice. Nature 441(7095):885–889. doi:10.1038/nature04724
28. Wang QJ, Ding Y, Kohtz DS, Mizushima N, Cristea IM, Rout MP, Chait BT, Zhong Y, Heintz N, Yue Z (2006) Induction of autophagy in axonal dystrophy and degeneration. J Neurosci 26(31):8057–8068. doi:10.1523/JNEUROSCI.2261-06.2006
29. Yang S, Zhang KY, Kariawasam R, Bax M, Fifita JA, Ooi L, Yerbury JJ, Nicholson GA, Blair IP (2015) Evaluation of skin fibroblasts from amyotrophic lateral sclerosis patients for the rapid study of pathological features. Neurotox Res 28(2):138–146. doi:10.1007/s12640-015-9532-1
30. Schneider CA, Rasband WS, Eliceiri KW (2012) NIH Image to ImageJ: 25 years of image analysis. Nat Methods 9(7):671–675
31. Zinchuk V, Zinchuk O, Okada T (2007) Quantitative colocalization analysis of multicolor confocal immunofluorescence microscopy images: pushing pixels to explore biological phenomena. Acta Histochem Cytochem 40(4):101–111. doi:10.1267/ahc.07002
32. N'Diaye EN, Kajihara KK, Hsieh I, Morisaki H, Debnath J, Brown EJ (2009) PLIC proteins or ubiquilins regulate autophagy-dependent cell survival during nutrient starvation. EMBO Rep 10(2):173–179. doi:10.1038/embor.2008.238
33. Klionsky DJ, Abdelmohsen K, Abe A, Abedin MJ, Abeliovich H, Acevedo Arozena A, Adachi H, Adams CM, Adams PD, Adeli K, Adhihetty PJ, Adler SG, Agam G, Agarwal R, Aghi MK, Agnello M, Agostinis P, Aguilar PV, Aguirre-Ghiso J, Airoldi EM, Ait-Si-Ali S, Akematsu T, Akporiaye ET, Al-Rubeai M, Albaiceta GM, Albanese C, Albani D, Albert ML, Aldudo J, Algul H, Alirezaei M, Alloza I, Almasan A, Almonte-Beceril M, Alnemri ES, Alonso C, Altan-Bonnet N, Altieri DC, Alvarez S, Alvarez-Erviti L, Alves S, Amadoro G, Amano A, Amantini C, Ambrosio S, Amelio I, Amer AO, Amessou M, Amon A, An Z, Anania FA, Andersen SU, Andley UP, Andreadi CK, Andrieu-Abadie N, Anel A, Ann DK, Anoopkumar-Dukie S, Antonioli M, Aoki H, Apostolova N, Aquila S, Aquilano K, Araki K, Arama E, Aranda A, Araya J, Arcaro A, Arias E, Arimoto H, Ariosa AR, Armstrong JL, Arnould T, Arsov I, Asanuma K, Askanas V, Asselin E, Atarashi R, Atherton SS, Atkin JD, Attardi LD, Auberger P, Auburger G, Aurelian L, Autelli R, Avagliano L, Avantaggiati ML, Avrahami L, Awale S, Azad N, Bachetti T, Backer JM, Bae DH, Bae JS, Bae ON, Bae SH, Baehrecke EH, Baek SH, Baghdiguian S, Bagniewska-Zadworna A, Bai H, Bai J, Bai XY, Bailly Y, Balaji KN, Balduini W, Ballabio A, Balzan R, Banerjee R, Banhegyi G, Bao H, Barbeau B, Barrachina MD, Barreiro E, Bartel B, Bartolome A, Bassham DC, Bassi MT, Bast RC, Jr., Basu A, Batista MT, Batoko H, Battino M, Bauckman K, Baumgarner BL, Bayer KU, Beale R, Beaulieu JF, Beck GR, Jr., Becker C, Beckham JD, Bedard PA, Bednarski PJ, Begley TJ, Behl C, Behrends C, Behrens GM, Behrns KE, Bejarano E, Belaid A, Belleudi F, Benard G, Berchem G, Bergamaschi D, Bergami M, Berkhout B, Berliocchi L, Bernard A, Bernard M, Bernassola F, Bertolotti A, Bess AS, Besteiro S, Bettuzzi S, Bhalla S, Bhattacharyya S, Bhutia SK, Biagosch C, Bianchi MW, Biard-Piechaczyk M, Billes V, Bincoletto C, Bingol B, Bird SW, Bitoun M, Bjedov I, Blackstone C, Blanc L, Blanco GA, Blomhoff HK, Boada-Romero E, Bockler S, Boes M, Boesze-Battaglia K, Boise LH, Bolino A, Boman A, Bonaldo P, Bordi M, Bosch J, Botana LM, Botti J, Bou G, Bouche M, Bouchecareilh M, Boucher MJ, Boulton ME, Bouret SG, Boya P, Boyer-Guittaut M, Bozhkov PV, Brady N, Braga VM, Brancolini C, Braus GH, Bravo-San Pedro JM, Brennan LA, Bresnick EH, Brest P, Bridges D, Bringer MA, Brini M, Brito GC, Brodin B, Brookes PS, Brown EJ, Brown K, Broxmeyer HE, Bruhat A, Brum PC, Brumell JH, Brunetti-Pierri N, Bryson-Richardson RJ, Buch S, Buchan AM, Budak H, Bulavin DV, Bultman SJ, Bultynck G, Bumbasirevic V, Burelle Y, Burke RE, Burmeister M, Butikofer P, Caberlotto L, Cadwell K, Cahova M, Cai D, Cai J, Cai Q, Calatayud S, Camougrand N, Campanella M, Campbell GR, Campbell M, Campello S, Candau R, Caniggia I, Cantoni L, Cao L, Caplan AB, Caraglia M, Cardinali C, Cardoso SM, Carew JS, Carleton LA, Carlin CR, Carloni S, Carlsson SR, Carmona-Gutierrez D, Carneiro LA, Carnevali O, Carra S, Carrier A, Carroll B, Casas C, Casas J, Cassinelli G, Castets P, Castro-Obregon S, Cavallini G, Ceccherini I, Cecconi F, Cederbaum AI, Cena V, Cenci S, Cerella C, Cervia D, Cetrullo S, Chaachouay H, Chae HJ, Chagin AS, Chai CY, Chakrabarti G, Chamilos G, Chan EY, Chan MT, Chandra D, Chandra P, Chang CP, Chang RC, Chang TY, Chatham JC, Chatterjee S, Chauhan S, Che Y, Cheetham ME, Cheluvappa R, Chen CJ, Chen G, Chen GC, Chen G, Chen H, Chen JW, Chen JK, Chen M, Chen M, Chen P, Chen Q, Chen Q, Chen SD, Chen S, Chen SS, Chen W, Chen WJ, Chen WQ, Chen W, Chen X, Chen YH, Chen YG, Chen Y, Chen Y, Chen Y, Chen YJ, Chen YQ, Chen Y, Chen Z, Chen Z, Cheng A, Cheng CH, Cheng H, Cheong H, Cherry S, Chesney J, Cheung CH, Chevet E, Chi HC, Chi SG, Chiacchiera F, Chiang HL, Chiarelli R, Chiariello M, Chieppa M, Chin LS, Chiong M, Chiu GN, Cho DH, Cho SG, Cho WC, Cho YY, Cho YS, Choi AM, Choi EJ, Choi EK, Choi J, Choi ME, Choi SI, Chou TF, Chouaib S, Choubey D, Choubey V, Chow KC, Chowdhury K, Chu CT, Chuang TH, Chun T, Chung H, Chung T, Chung YL, Chwae YJ, Cianfanelli V, Ciarcia R, Ciechomska IA, Ciriolo MR, Cirone M, Claerhout S, Clague MJ, Claria J, Clarke PG, Clarke R, Clementi E, Cleyrat C, Cnop M, Coccia EM, Cocco T, Codogno P, Coers J, Cohen EE, Colecchia D, Coletto L, Coll NS, Colucci-Guyon E, Comincini S, Condello M, Cook KL, Coombs GH, Cooper CD, Cooper JM, Coppens I, Corasaniti MT, Corazzari M, Corbalan R, Corcelle-Termeau E, Cordero MD, Corral-Ramos C, Corti O, Cossarizza A, Costelli P, Costes S, Cotman SL, Coto-Montes A, Cottet S, Couve E, Covey LR, Cowart LA, Cox JS, Coxon FP, Coyne CB, Cragg MS, Craven RJ, Crepaldi T, Crespo JL, Criollo A, Crippa V, Cruz MT, Cuervo AM, Cuezva JM, Cui T, Cutillas PR, Czaja MJ, Czyzyk-Krzeska MF, Dagda RK, Dahmen U, Dai C, Dai W, Dai Y, Dalby KN, Dalla Valle L, Dalmasso G, D'Amelio M, Damme M, Darfeuille-Michaud A, Dargemont C, Darley-Usmar VM, Dasarathy S, Dasgupta B, Dash S, Dass CR, Davey HM, Davids LM, Davila D, Davis RJ, Dawson TM, Dawson VL, Daza P, de Belleroche J, de Figueiredo P, de Figueiredo RC, de la Fuente J, De Martino L, De Matteis A, De Meyer GR, De Milito A, De Santi M, de Souza W, De Tata V, De Zio D, Debnath J, Dechant R, Decuypere JP, Deegan S, Dehay B, Del Bello B, Del Re DP, Delage-Mourroux R, Delbridge LM, Deldicque L,

Delorme-Axford E, Deng Y, Dengjel J, Denizot M, Dent P, Der CJ, Deretic V, Derrien B, Deutsch E, Devarenne TP, Devenish RJ, Di Bartolomeo S, Di Daniele N, Di Domenico F, Di Nardo A, Di Paola S, Di Pietro A, Di Renzo L, DiAntonio A, Diaz-Araya G, Diaz-Laviada I, Diaz-Meco MT, Diaz-Nido J, Dickey CA, Dickson RC, Diederich M, Digard P, Dikic I, Dinesh-Kumar SP, Ding C, Ding WX, Ding Z, Dini L, Distler JH, Diwan A, Djavaheri-Mergny M, Dmytruk K, Dobson RC, Doetsch V, Dokladny K, Dokudovskaya S, Donadelli M, Dong XC, Dong X, Dong Z, Donohue TM, Jr., Doran KS, D'Orazi G, Dorn GW, 2nd, Dosenko V, Dridi S, Drucker L, Du J, Du LL, Du L, du Toit A, Dua P, Duan L, Duann P, Dubey VK, Duchen MR, Duchosal MA, Duez H, Dugail I, Dumit VI, Duncan MC, Dunlop EA, Dunn WA, Jr., Dupont N, Dupuis L, Duran RV, Durcan TM, Duvezin-Caubet S, Duvvuri U, Eapen V, Ebrahimi-Fakhari D, Echard A, Eckhart L, Edelstein CL, Edinger AL, Eichinger L, Eisenberg T, Eisenberg-Lerner A, Eissa NT, El-Deiry WS, El-Khoury V, Elazar Z, Eldar-Finkelman H, Elliott CJ, Emanuele E, Emmenegger U, Engedal N, Engelbrecht AM, Engelender S, Enserink JM, Erdmann R, Erenpreisa J, Eri R, Eriksen JL, Erman A, Escalante R, Eskelinen EL, Espert L, Esteban-Martinez L, Evans TJ, Fabri M, Fabrias G, Fabrizi C, Facchiano A, Faergeman NJ, Faggioni A, Fairlie WD, Fan C, Fan D, Fan J, Fang S, Fanto M, Fanzani A, Farkas T, Faure M, Favier FB, Fearnhead H, Federici M, Fei E, Felizardo TC, Feng H, Feng Y, Feng Y, Ferguson TA, Fernandez AF, Fernandez-Barrena MG, Fernandez-Checa JC, Fernandez-Lopez A, Fernandez-Zapico ME, Feron O, Ferraro E, Ferreira-Halder CV, Fesus L, Feuer R, Fiesel FC, Filippi-Chiela EC, Filomeni G, Fimia GM, Fingert JH, Finkbeiner S, Finkel T, Fiorito F, Fisher PB, Flajolet M, Flamigni F, Florey O, Florio S, Floto RA, Folini M, Follo C, Fon EA, Fornai F, Fortunato F, Fraldi A, Franco R, Francois A, Francois A, Frankel LB, Fraser ID, Frey N, Freyssenet DG, Frezza C, Friedman SL, Frigo DE, Fu D, Fuentes JM, Fueyo J, Fujitani Y, Fujiwara Y, Fujiya M, Fukuda M, Fulda S, Fusco C, Gabryel B, Gaestel M, Gailly P, Gajewska M, Galadari S, Galili G, Galindo I, Galindo MF, Galliciotti G, Galluzzi L, Galluzzi L, Galy V, Gammoh N, Gandy S, Ganesan AK, Ganesan S, Ganley IG, Gannage M, Gao FB, Gao F, Gao JX, Garcia Nannig L, Garcia Vescovi E, Garcia-Macia M, Garcia-Ruiz C, Garg AD, Garg PK, Gargini R, Gassen NC, Gatica D, Gatti E, Gavard J, Gavathiotis E, Ge L, Ge P, Ge S, Gean PW, Gelmetti V, Genazzani AA, Geng J, Genschik P, Gerner L, Gestwicki JE, Gewirtz DA, Ghavami S, Ghigo E, Ghosh D, Giammarioli AM, Giampieri F, Giampietri C, Giatromanolaki A, Gibbings DJ, Gibellini L, Gibson SB, Ginet V, Giordano A, Giorgini F, Giovannetti E, Girardin SE, Gispert S, Giuliano S, Gladson CL, Glavic A, Gleave M, Godefroy N, Gogal RM, Jr., Gokulan K, Goldman GH, Goletti D, Goligorsky MS, Gomes AV, Gomes LC, Gomez H, Gomez-Manzano C, Gomez-Sanchez R, Goncalves DA, Goncu E, Gong Q, Gongora C, Gonzalez CB, Gonzalez-Alegre P, Gonzalez-Cabo P, Gonzalez-Polo RA, Goping IS, Gorbea C, Gorbunov NV, Goring DR, Gorman AM, Gorski SM, Goruppi S, Goto-Yamada S, Gotor C, Gottlieb RA, Gozes I, Gozuacik D, Graba Y, Graef M, Granato GE, Grant GD, Grant S, Gravina GL, Green DR, Greenhough A, Greenwood MT, Grimaldi B, Gros F, Grose C, Groulx JF, Gruber F, Grumati P, Grune T, Guan JL, Guan KL, Guerra B, Guillen C, Gulshan K, Gunst J, Guo C, Guo L, Guo M, Guo W, Guo XG, Gust AA, Gustafsson AB, Gutierrez E, Gutierrez MG, Gwak HS, Haas A, Haber JE, Hadano S, Hagedorn M, Hahn DR, Halayko AJ, Hamacher-Brady A, Hamada K, Hamai A, Hamann A, Hamasaki M, Hamer I, Hamid Q, Hammond EM, Han F, Han W, Handa JT, Hanover JA, Hansen M, Harada M, Harhaji-Trajkovic L, Harper JW, Harrath AH, Harris AL, Harris J, Hasler U, Hasselblatt P, Hasui K, Hawley RG, Hawley TS, He C, He CY, He F, He G, He RR, He XH, He YW, He YY, Heath JK, Hebert MJ, Heinzen RA, Helgason GV, Hensel M, Henske EP, Her C, Herman PK, Hernandez A, Hernandez C, Hernandez-Tiedra S, Hetz C, Hiesinger PR, Higaki K, Hilfiker S, Hill BG, Hill JA, Hill WD, Hino K, Hofius D, Hofman P, Hoglinger GU, Hohfeld J, Holz MK, Hong Y, Hood DA, Hoozemans JJ, Hoppe T, Hsu C, Hsu CY, Hsu LC, Hu D, Hu G, Hu HM, Hu H, Hu MC, Hu YC, Hu ZW, Hua F, Hua Y, Huang C, Huang HL, Huang KH, Huang KY, Huang S, Huang S, Huang WP, Huang YR, Huang Y, Huang Y, Huber TB, Huebbe P, Huh WK, Hulmi JJ, Hur GM, Hurley JH, Husak Z, Hussain SN, Hussain S, Hwang JJ, Hwang S, Hwang TI, Ichihara A, Imai Y, Imbriano C, Inomata M, Into T, Iovane V, Iovanna JL, Iozzo RV, Ip NY, Irazoqui JE, Iribarren P, Isaka Y, Isakovic AJ, Ischiropoulos H, Isenberg JS, Ishaq M, Ishida H, Ishii I, Ishmael JE, Isidoro C, Isobe K, Isono E, Issazadeh-Navikas S, Itahana K, Itakura E, Ivanov AI, Iyer AK, Izquierdo JM, Izumi Y, Izzo V, Jaattela M, Jaber N, Jackson DJ, Jackson WT, Jacob TG, Jacques TS, Jagannath C, Jain A, Jana NR, Jang BK, Jani A, Janji B, Jannig PR, Jansson PJ, Jean S, Jendrach M, Jeon JH, Jessen N, Jeung EB, Jia K, Jia L, Jiang H, Jiang H, Jiang L, Jiang T, Jiang X, Jiang X, Jiang X, Jiang Y, Jiang Y, Jimenez A, Jin C, Jin H, Jin L, Jin M, Jin S, Jinwal UK, Jo EK, Johansen T, Johnson DE, Johnson GV, Johnson JD, Jonasch E, Jones C, Joosten LA, Jordan J, Joseph AM, Joseph B, Joubert AM, Ju D, Ju J, Juan HF, Juenemann K, Juhasz G, Jung HS, Jung JU, Jung YK, Jungbluth H, Justice MJ, Jutten B, Kaakoush NO, Kaarniranta K, Kaasik A, Kabuta T, Kaeffer B, Kagedal K, Kahana A, Kajimura S, Kakhlon O, Kalia M, Kalvakolanu DV, Kamada Y, Kambas K, Kaminskyy VO, Kampinga HH, Kandouz M, Kang C, Kang R, Kang TC, Kanki T, Kanneganti TD, Kanno H, Kanthasamy AG, Kantorow M, Kaparakis-Liaskos M, Kapuy O, Karantza V, Karim MR, Karmakar P, Kaser A, Kaushik S, Kawula T, Kaynar AM, Ke PY, Ke ZJ, Kehrl JH, Keller KE, Kemper JK, Kenworthy AK, Kepp O, Kern A, Kesari S, Kessel D, Ketteler R, Kettelhut Ido C, Khambu B, Khan MM, Khandelwal VK, Khare S, Kiang JG, Kiger AA, Kihara A, Kim AL, Kim CH, Kim DR, Kim DH, Kim EK, Kim HY, Kim HR, Kim JS, Kim JH, Kim JC, Kim JH, Kim KW, Kim MD, Kim MM, Kim PK, Kim SW, Kim SY, Kim YS, Kim Y, Kimchi A, Kimmelman AC, Kimura T, King JS, Kirkegaard K, Kirkin V, Kirshenbaum LA, Kishi S, Kitajima Y, Kitamoto K, Kitaoka Y, Kitazato K, Kley RA, Klimecki WT, Klinkenberg M, Klucken J, Knaevelsrud H, Knecht E, Knuppertz L, Ko JL, Kobayashi S, Koch JC, Koechlin-Ramonatxo C, Koenig U, Koh YH, Kohler K, Kohlwein SD, Koike M, Komatsu M, Kominami E, Kong D, Kong HJ, Konstantakou EG, Kopp BT, Korcsmaros T, Korhonen L, Korolchuk VI, Koshkina NV, Kou Y, Koukourakis MI, Koumenis C, Kovacs AL, Kovacs T, Kovacs WJ, Koya D, Kraft C, Krainc D, Kramer H, Kravic-Stevovic T, Krek W, Kretz-Remy C, Krick R, Krishnamurthy M, Kriston-Vizi J, Kroemer G, Kruer MC, Kruger R, Ktistakis NT, Kuchitsu K, Kuhn C, Kumar AP, Kumar A, Kumar A, Kumar D, Kumar D, Kumar R, Kumar S, Kundu M, Kung HJ, Kuno A, Kuo SH, Kuret J, Kurz T, Kwok T, Kwon TK, Kwon YT, Kyrmizi I, La Spada AR, Lafont F, Lahm T, Lakkaraju A, Lam T, Lamark T, Lancel S, Landowski TH, Lane DJ, Lane JD, Lanzi C, Lapaquette P, Lapierre LR, Laporte J, Laukkarinen J, Laurie GW, Lavandero S, Lavie L, LaVoie MJ, Law BY, Law HK, Law KB, Layfield R, Lazo PA, Le Cam L, Le Roch KG, Le Stunff H, Leardkamolkarn V, Lecuit M, Lee BH, Lee CH, Lee EF, Lee GM, Lee HJ, Lee H, Lee JK, Lee J, Lee JH, Lee JH, Lee M, Lee MS, Lee PJ, Lee SW, Lee SJ, Lee SJ, Lee SY, Lee SH, Lee SS, Lee SJ, Lee S, Lee YR, Lee YJ, Lee YH, Leeuwenburgh C, Lefort S, Legouis R, Lei J, Lei QY, Leib DA, Leibowitz G, Lekli I, Lemaire SD, Lemasters JJ, Lemberg MK, Lemoine A, Leng S, Lenz G, Lenzi P, Lerman LO, Lettieri Barbato D, Leu JI, Leung HY, Levine

B, Lewis PA, Lezoualc'h F, Li C, Li F, Li FJ, Li J, Li K, Li L, Li M, Li M, Li Q, Li R, Li S, Li W, Li W, Li X, Li Y, Lian J, Liang C, Liang Q, Liao Y, Liberal J, Liberski PP, Lie P, Lieberman AP, Lim HJ, Lim KL, Lim K, Lima RT, Lin CS, Lin CF, Lin F, Lin F, Lin FC, Lin K, Lin KH, Lin PH, Lin T, Lin WW, Lin YS, Lin Y, Linden R, Lindholm D, Lindqvist LM, Lingor P, Linkermann A, Liotta LA, Lipinski MM, Lira VA, Lisanti MP, Liton PB, Liu B, Liu C, Liu CF, Liu F, Liu HJ, Liu J, Liu JJ, Liu JL, Liu K, Liu L, Liu L, Liu Q, Liu RY, Liu S, Liu S, Liu W, Liu XD, Liu X, Liu XH, Liu X, Liu X, Liu X, Liu Y, Liu Y, Liu Z, Liu Z, Liuzzi JP, Lizard G, Ljujic M, Lodhi IJ, Logue SE, Lokeshwar BL, Long YC, Lonial S, Loos B, Lopez-Otin C, Lopez-Vicario C, Lorente M, Lorenzi PL, Lorincz P, Los M, Lotze MT, Lovat PE, Lu B, Lu B, Lu J, Lu Q, Lu SM, Lu S, Lu Y, Luciano F, Luckhart S, Lucocq JM, Ludovico P, Lugea A, Lukacs NW, Lum JJ, Lund AH, Luo H, Luo J, Luo S, Luparello C, Lyons T, Ma J, Ma Y, Ma Y, Ma Z, Machado J, Machado-Santelli GM, Macian F, MacIntosh GC, MacKeigan JP, Macleod KF, MacMicking JD, MacMillan-Crow LA, Madeo F, Madesh M, Madrigal-Matute J, Maeda A, Maeda T, Maegawa G, Maellaro E, Maes H, Magarinos M, Maiese K, Maiti TK, Maiuri L, Maiuri MC, Maki CG, Malli R, Malorni W, Maloyan A, Mami-Chouaib F, Man N, Mancias JD, Mandelkow EM, Mandell MA, Manfredi AA, Manie SN, Manzoni C, Mao K, Mao Z, Mao ZW, Marambaud P, Marconi AM, Marelja Z, Marfe G, Margeta M, Margittai E, Mari M, Mariani FV, Marin C, Marinelli S, Marino G, Markovic I, Marquez R, Martelli AM, Martens S, Martin KR, Martin SJ, Martin S, Martin-Acebes MA, Martin-Sanz P, Martinand-Mari C, Martinet W, Martinez J, Martinez-Lopez N, Martinez-Outschoorn U, Martinez-Velazquez M, Martinez-Vicente M, Martins WK, Mashima H, Mastrianni JA, Matarese G, Matarrese P, Mateo R, Matoba S, Matsumoto N, Matsushita T, Matsuura A, Matsuzawa T, Mattson MP, Matus S, Maugeri N, Mauvezin C, Mayer A, Maysinger D, Mazzolini GD, McBrayer MK, McCall K, McCormick C, McInerney GM, McIver SC, McKenna S, McMahon JJ, McNeish IA, Mechta-Grigoriou F, Medema JP, Medina DL, Megyeri K, Mehrpour M, Mehta JL, Mei Y, Meier UC, Meijer AJ, Melendez A, Melino G, Melino S, de Melo EJ, Mena MA, Meneghini MD, Menendez JA, Menezes R, Meng L, Meng LH, Meng S, Menghini R, Menko AS, Menna-Barreto RF, Menon MB, Meraz-Rios MA, Merla G, Merlini L, Merlot AM, Meryk A, Meschini S, Meyer JN, Mi MT, Miao CY, Micale L, Michaeli S, Michiels C, Migliaccio AR, Mihailidou AS, Mijaljica D, Mikoshiba K, Milan E, Miller-Fleming L, Mills GB, Mills IG, Minakaki G, Minassian BA, Ming XF, Minibayeva F, Minina EA, Mintern JD, Minucci S, Miranda-Vizuete A, Mitchell CH, Miyamoto S, Miyazawa K, Mizushima N, Mnich K, Mograbi B, Mohseni S, Moita LF, Molinari M, Molinari M, Moller AB, Mollereau B, Mollinedo F, Mongillo M, Monick MM, Montagnaro S, Montell C, Moore DJ, Moore MN, Mora-Rodriguez R, Moreira PI, Morel E, Morelli MB, Moreno S, Morgan MJ, Moris A, Moriyasu Y, Morrison JL, Morrison LA, Morselli E, Moscat J, Moseley PL, Mostowy S, Motori E, Mottet D, Mottram JC, Moussa CE, Mpakou VE, Mukhtar H, Mulcahy Levy JM, Muller S, Munoz-Moreno R, Munoz-Pinedo C, Munz C, Murphy ME, Murray JT, Murthy A, Mysorekar IU, Nabi IR, Nabissi M, Nader GA, Nagahara Y, Nagai Y, Nagata K, Nagelkerke A, Nagy P, Naidu SR, Nair S, Nakano H, Nakatogawa H, Nanjundan M, Napolitano G, Naqvi NI, Nardacci R, Narendra DP, Narita M, Nascimbeni AC, Natarajan R, Navegantes LC, Nawrocki ST, Nazarko TY, Nazarko VY, Neill T, Neri LM, Netea MG, Netea-Maier RT, Neves BM, Ney PA, Nezis IP, Nguyen HT, Nguyen HP, Nicot AS, Nilsen H, Nilsson P, Nishimura M, Nishino I, Niso-Santano M, Niu H, Nixon RA, Njar VC, Noda T, Noegel AA, Nolte EM, Norberg E, Norga KK, Noureini SK, Notomi S, Notterpek L, Nowikovsky K, Nukina N, Nurnberger T, O'Donnell VB, O'Donovan T, O'Dwyer PJ, Oehme I, Oeste CL, Ogawa M, Ogretmen B, Ogura Y, Oh YJ, Ohmuraya M, Ohshima T, Ojha R, Okamoto K, Okazaki T, Oliver FJ, Ollinger K, Olsson S, Orban DP, Ordonez P, Orhon I, Orosz L, O'Rourke EJ, Orozco H, Ortega AL, Ortona E, Osellame LD, Oshima J, Oshima S, Osiewacz HD, Otomo T, Otsu K, Ou JH, Outeiro TF, Ouyang DY, Ouyang H, Overholtzer M, Ozbun MA, Ozdinler PH, Ozpolat B, Pacelli C, Paganetti P, Page G, Pages G, Pagnini U, Pajak B, Pak SC, Pakos-Zebrucka K, Pakpour N, Palkova Z, Palladino F, Pallauf K, Pallet N, Palmieri M, Paludan SR, Palumbo C, Palumbo S, Pampliega O, Pan H, Pan W, Panaretakis T, Pandey A, Pantazopoulou A, Papackova Z, Papademetrio DL, Papassideri I, Papini A, Parajuli N, Pardo J, Parekh VV, Parenti G, Park JI, Park J, Park OK, Parker R, Parlato R, Parys JB, Parzych KR, Pasquet JM, Pasquier B, Pasumarthi KB, Patschan D, Patterson C, Pattingre S, Pattison S, Pause A, Pavenstadt H, Pavone F, Pedrozo Z, Pena FJ, Penalva MA, Pende M, Peng J, Penna F, Penninger JM, Pensalfini A, Pepe S, Pereira GJ, Pereira PC, Perez-de la Cruz V, Perez-Perez ME, Perez-Rodriguez D, Perez-Sala D, Perier C, Perl A, Perlmutter DH, Perrotta I, Pervaiz S, Pesonen M, Pessin JE, Peters GJ, Petersen M, Petrache I, Petrof BJ, Petrovski G, Phang JM, Piacentini M, Pierdominici M, Pierre P, Pierrefite-Carle V, Pietrocola F, Pimentel-Muinos FX, Pinar M, Pineda B, Pinkas-Kramarski R, Pinti M, Pinton P, Piperdi B, Piret JM, Platanias LC, Platta HW, Plowey ED, Poggeler S, Poirot M, Polcic P, Poletti A, Poon AH, Popelka H, Popova B, Poprawa I, Poulose SM, Poulton J, Powers SK, Powers T, Pozuelo-Rubio M, Prak K, Prange R, Prescott M, Priault M, Prince S, Proia RL, Proikas-Cezanne T, Prokisch H, Promponas VJ, Przyklenk K, Puertollano R, Pugazhenthi S, Puglielli L, Pujol A, Puyal J, Pyeon D, Qi X, Qian WB, Qin ZH, Qiu Y, Qu Z, Quadrilatero J, Quinn F, Raben N, Rabinowich H, Radogna F, Ragusa MJ, Rahmani M, Raina K, Ramanadham S, Ramesh R, Rami A, Randall-Demllo S, Randow F, Rao H, Rao VA, Rasmussen BB, Rasse TM, Ratovitski EA, Rautou PE, Ray SK, Razani B, Reed BH, Reggiori F, Rehm M, Reichert AS, Rein T, Reiner DJ, Reits E, Ren J, Ren X, Renna M, Reusch JE, Revuelta JL, Reyes L, Rezaie AR, Richards RI, Richardson DR, Richetta C, Riehle MA, Rihn BH, Rikihisa Y, Riley BE, Rimbach G, Rippo MR, Ritis K, Rizzi F, Rizzo E, Roach PJ, Robbins J, Roberge M, Roca G, Roccheri MC, Rocha S, Rodrigues CM, Rodriguez CI, de Cordoba SR, Rodriguez-Muela N, Roelofs J, Rogov VV, Rohn TT, Rohrer B, Romanelli D, Romani L, Romano PS, Roncero MI, Rosa JL, Rosello A, Rosen KV, Rosenstiel P, Rost-Roszkowska M, Roth KA, Roue G, Rouis M, Rouschop KM, Ruan DT, Ruano D, Rubinsztein DC, Rucker EB, 3rd, Rudich A, Rudolf E, Rudolf R, Ruegg MA, Ruiz-Roldan C, Ruparelia AA, Rusmini P, Russ DW, Russo GL, Russo G, Russo R, Rusten TE, Ryabovol V, Ryan KM, Ryter SW, Sabatini DM, Sacher M, Sachse C, Sack MN, Sadoshima J, Saftig P, Sagi-Eisenberg R, Sahni S, Saikumar P, Saito T, Saitoh T, Sakakura K, Sakoh-Nakatogawa M, Sakuraba Y, Salazar-Roa M, Salomoni P, Saluja AK, Salvaterra PM, Salvioli R, Samali A, Sanchez AM, Sanchez-Alcazar JA, Sanchez-Prieto R, Sandri M, Sanjuan MA, Santaguida S, Santambrogio L, Santoni G, Dos Santos CN, Saran S, Sardiello M, Sargent G, Sarkar P, Sarkar S, Sarrias MR, Sarwal MM, Sasakawa C, Sasaki M, Sass M, Sato K, Sato M, Satriano J, Savaraj N, Saveljeva S, Schaefer L, Schaible UE, Scharl M, Schatzl HM, Schekman R, Scheper W, Schiavi A, Schipper HM, Schmeisser H, Schmidt J, Schmitz I, Schneider BE, Schneider EM, Schneider JL, Schon EA, Schonenberger MJ, Schonthal AH, Schorderet DF, Schroder B, Schuck S, Schulze RJ, Schwarten M, Schwarz TL, Sciarretta S, Scotto K, Scovassi AI, Screaton RA, Screen M, Seca H, Sedej S, Segatori L, Segev N, Seglen PO, Segui-Simarro JM,

Segura-Aguilar J, Seki E, Sell C, Seiliez I, Semenkovich CF, Semenza GL, Sen U, Serra AL, Serrano-Puebla A, Sesaki H, Setoguchi T, Settembre C, Shacka JJ, Shajahan-Haq AN, Shapiro IM, Sharma S, She H, Shen CK, Shen CC, Shen HM, Shen S, Shen W, Sheng R, Sheng X, Sheng ZH, Shepherd TG, Shi J, Shi Q, Shi Q, Shi Y, Shibutani S, Shibuya K, Shidoji Y, Shieh JJ, Shih CM, Shimada Y, Shimizu S, Shin DW, Shinohara ML, Shintani M, Shintani T, Shioi T, Shirabe K, Shiri-Sverdlov R, Shirihai O, Shore GC, Shu CW, Shukla D, Sibirny AA, Sica V, Sigurdson CJ, Sigurdsson EM, Sijwali PS, Sikorska B, Silveira WA, Silvente-Poirot S, Silverman GA, Simak J, Simmet T, Simon AK, Simon HU, Simone C, Simons M, Simonsen A, Singh R, Singh SV, Singh SK, Sinha D, Sinha S, Sinicrope FA, Sirko A, Sirohi K, Sishi BJ, Sittler A, Siu PM, Sivridis E, Skwarska A, Slack R, Slaninova I, Slavov N, Smaili SS, Smalley KS, Smith DR, Soenen SJ, Soleimanpour SA, Solhaug A, Somasundaram K, Son JH, Sonawane A, Song C, Song F, Song HK, Song JX, Song W, Soo KY, Sood AK, Soong TW, Soontornniyomkij V, Sorice M, Sotgia F, Soto-Pantoja DR, Sotthibundhu A, Sousa MJ, Spaink HP, Span PN, Spang A, Sparks JD, Speck PG, Spector SA, Spies CD, Springer W, Clair DS, Stacchiotti A, Staels B, Stang MT, Starczynowski DT, Starokadomskyy P, Steegborn C, Steele JW, Stefanis L, Steffan J, Stellrecht CM, Stenmark H, Stepkowski TM, Stern ST, Stevens C, Stockwell BR, Stoka V, Storchova Z, Stork B, Stratoulias V, Stravopodis DJ, Strnad P, Strohecker AM, Strom AL, Stromhaug P, Stulik J, Su YX, Su Z, Subauste CS, Subramaniam S, Sue CM, Suh SW, Sui X, Sukseree S, Sulzer D, Sun FL, Sun J, Sun J, Sun SY, Sun Y, Sun Y, Sun Y, Sundaramoorthy V, Sung J, Suzuki H, Suzuki K, Suzuki N, Suzuki T, Suzuki YJ, Swanson MS, Swanton C, Sward K, Swarup G, Sweeney ST, Sylvester PW, Szatmari Z, Szegezdi E, Szlosarek PW, Taegtmeyer H, Tafani M, Taillebourg E, Tait SW, Takacs-Vellai K, Takahashi Y, Takats S, Takemura G, Takigawa N, Talbot NJ, Tamagno E, Tamburini J, Tan CP, Tan L, Tan ML, Tan M, Tan YJ, Tanaka K, Tanaka M, Tang D, Tang D, Tang G, Tanida I, Tanji K, Tannous BA, Tapia JA, Tasset-Cuevas I, Tatar M, Tavassoly I, Tavernarakis N, Taylor A, Taylor GS, Taylor GA, Taylor JP, Taylor MJ, Tchetina EV, Tee AR, Teixeira-Clerc F, Telang S, Tencomnao T, Teng BB, Teng RJ, Terro F, Tettamanti G, Theiss AL, Theron AE, Thomas KJ, Thome MP, Thomes PG, Thorburn A, Thorner J, Thum T, Thumm M, Thurston TL, Tian L, Till A, Ting JP, Titorenko VI, Toker L, Toldo S, Tooze SA, Topisirovic I, Torgersen ML, Torosantucci L, Torriglia A, Torrisi MR, Tournier C, Towns R, Trajkovic V, Travassos LH, Triola G, Tripathi DN, Trisciuoglio D, Troncoso R, Trougakos IP, Truttmann AC, Tsai KJ, Tschan MP, Tseng YH, Tsukuba T, Tsung A, Tsvetkov AS, Tu S, Tuan HY, Tucci M, Tumbarello DA, Turk B, Turk V, Turner RF, Tveita AA, Tyagi SC, Ubukata M, Uchiyama Y, Udelnow A, Ueno T, Umekawa M, Umemiya-Shirafuji R, Underwood BR, Ungermann C, Ureshino RP, Ushioda R, Uversky VN, Uzcategui NL, Vaccari T, Vaccaro MI, Vachova L, Vakifahmetoglu-Norberg H, Valdor R, Valente EM, Vallette F, Valverde AM, Van den Berghe G, Van Den Bosch L, van den Brink GR, van der Goot FG, van der Klei IJ, van der Laan LJ, van Doorn WG, van Egmond M, van Golen KL, Van Kaer L, van Lookeren Campagne M, Vandenabeele P, Vandenberghe W, Vanhorebeek I, Varela-Nieto I, Vasconcelos MH, Vasko R, Vavvas DG, Vega-Naredo I, Velasco G, Velentzas AD, Velentzas PD, Vellai T, Vellenga E, Vendelbo MH, Venkatachalam K, Ventura N, Ventura S, Veras PS, Verdier M, Vertessy BG, Viale A, Vidal M, Vieira HL, Vierstra RD, Vigneswaran N, Vij N, Vila M, Villar M, Villar VH, Villarroya J, Vindis C, Viola G, Viscomi MT, Vitale G, Vogl DT, Voitsekhovskaja OV, von Haefen C, von Schwarzenberg K, Voth DE, Vouret-Craviari V, Vuori K, Vyas JM, Waeber C, Walker CL, Walker MJ, Walter J, Wan L, Wan X, Wang B, Wang C, Wang CY, Wang C, Wang C, Wang C, Wang D, Wang F, Wang F, Wang G, Wang HJ, Wang H, Wang HG, Wang H, Wang HD, Wang J, Wang J, Wang M, Wang MQ, Wang PY, Wang P, Wang RC, Wang S, Wang TF, Wang X, Wang XJ, Wang XW, Wang X, Wang X, Wang Y, Wang Y, Wang Y, Wang YJ, Wang Y, Wang Y, Wang YT, Wang Y, Wang ZN, Wappner P, Ward C, Ward DM, Warnes G, Watada H, Watanabe Y, Watase K, Weaver TE, Weekes CD, Wei J, Weide T, Weihl CC, Weindl G, Weis SN, Wen L, Wen X, Wen Y, Westermann B, Weyand CM, White AR, White E, Whitton JL, Whitworth AJ, Wiels J, Wild F, Wildenberg ME, Wileman T, Wilkinson DS, Wilkinson S, Willbold D, Williams C, Williams K, Williamson PR, Winklhofer KF, Witkin SS, Wohlgemuth SE, Wollert T, Wolvetang EJ, Wong E, Wong GW, Wong RW, Wong VK, Woodcock EA, Wright KL, Wu C, Wu D, Wu GS, Wu J, Wu J, Wu M, Wu M, Wu S, Wu WK, Wu Y, Wu Z, Xavier CP, Xavier RJ, Xia GX, Xia T, Xia W, Xia Y, Xiao H, Xiao J, Xiao S, Xiao W, Xie CM, Xie Z, Xie Z, Xilouri M, Xiong Y, Xu C, Xu C, Xu F, Xu H, Xu H, Xu J, Xu J, Xu J, Xu L, Xu X, Xu Y, Xu Y, Xu ZX, Xu Z, Xue Y, Yamada T, Yamamoto A, Yamanaka K, Yamashina S, Yamashiro S, Yan B, Yan B, Yan X, Yan Z, Yanagi Y, Yang DS, Yang JM, Yang L, Yang M, Yang PM, Yang P, Yang Q, Yang W, Yang WY, Yang X, Yang Y, Yang Y, Yang Z, Yang Z, Yao MC, Yao PJ, Yao X, Yao Z, Yao Z, Yasui LS, Ye M, Yedvobnick B, Yeganeh B, Yeh ES, Yeyati PL, Yi F, Yi L, Yin XM, Yip CK, Yoo YM, Yoo YH, Yoon SY, Yoshida K, Yoshimori T, Young KH, Yu H, Yu JJ, Yu JT, Yu J, Yu L, Yu WH, Yu XF, Yu Z, Yuan J, Yuan ZM, Yue BY, Yue J, Yue Z, Zacks DN, Zacksenhaus E, Zaffaroni N, Zaglia T, Zakeri Z, Zecchini V, Zeng J, Zeng M, Zeng Q, Zervos AS, Zhang DD, Zhang F, Zhang G, Zhang GC, Zhang H, Zhang H, Zhang H, Zhang H, Zhang J, Zhang J, Zhang J, Zhang J, Zhang JP, Zhang L, Zhang L, Zhang L, Zhang L, Zhang MY, Zhang X, Zhang XD, Zhang Y, Zhang Y, Zhang Y, Zhang Y, Zhang Y, Zhao M, Zhao WL, Zhao X, Zhao YG, Zhao Y, Zhao Y, Zhao YX, Zhao Z, Zhao ZJ, Zheng D, Zheng XL, Zheng X, Zhivotovsky B, Zhong Q, Zhou GZ, Zhou G, Zhou H, Zhou SF, Zhou XJ, Zhu H, Zhu H, Zhu WG, Zhu W, Zhu XF, Zhu Y, Zhuang SM, Zhuang X, Ziparo E, Zois CE, Zoladek T, Zong WX, Zorzano A, Zughaier SM (2016) Guidelines for the use and interpretation of assays for monitoring autophagy (3rd edition). Autophagy 12(1):1–222. doi:10.1080/15548627.2015.1100356

34. Ganay T, Boizot A, Burrer R, Chauvin JP, Bomont P (2011) Sensory-motor deficits and neurofilament disorganization in gigaxonin-null mice. Mol Neurodegeneration 6:25. doi:10.1186/1750-1326-6-25
35. Hebron ML, Lonskaya I, Sharpe K, Weerasinghe PP, Algarzae NK, Shekoyan AR, Moussa CE (2013) Parkin ubiquitinates Tar-DNA binding protein-43 (TDP-43) and promotes its cytosolic accumulation via interaction with histone deacetylase 6 (HDAC6). J Biol Chem 288(6):4103–4115. doi:10.1074/jbc.M112.419945
36. Ishigaki S, Hishikawa N, Niwa J, Iemura S, Natsume T, Hori S, Kakizuka A, Tanaka K, Sobue G (2004) Physical and functional interaction between Dorfin and Valosin-containing protein that are colocalized in ubiquitylated inclusions in neurodegenerative disorders. J Biol Chem 279(49):51376–51385. doi:10.1074/jbc.M406683200
37. Williams AJ, Knutson TM, Colomer Gould VF, Paulson HL (2009) In vivo suppression of polyglutamine neurotoxicity by C-terminus of Hsp70-interacting protein (CHIP) supports an aggregation model of pathogenesis. Neurobiol Dis 33(3):342–353. doi:10.1016/j.nbd.2008.10.016
38. Cuervo AM, Wong E (2014) Chaperone-mediated autophagy: roles in disease and aging. Cell Res 24(1):92–104. doi:10.1038/cr.2013.153

39. Mizushima N (2007) Autophagy: process and function. Genes Dev 21(22):2861–2873. doi:10.1101/gad.1599207
40. Mizushima N, Yoshimori T (2007) How to interpret LC3 immunoblotting. Autophagy 3(6):542–545
41. Komatsu M, Waguri S, Koike M, Sou YS, Ueno T, Hara T, Mizushima N, Iwata J, Ezaki J, Murata S, Hamazaki J, Nishito Y, Iemura S, Natsume T, Yanagawa T, Uwayama J, Warabi E, Yoshida H, Ishii T, Kobayashi A, Yamamoto M, Yue Z, Uchiyama Y, Kominami E, Tanaka K (2007) Homeostatic levels of p62 control cytoplasmic inclusion body formation in autophagy-deficient mice. Cell 131(6):1149–1163. doi:10.1016/j.cell.2007.10.035
42. Filimonenko M, Stuffers S, Raiborg C, Yamamoto A, Malerod L, Fisher EM, Isaacs A, Brech A, Stenmark H, Simonsen A (2007) Functional multivesicular bodies are required for autophagic clearance of protein aggregates associated with neurodegenerative disease. J Cell Biol 179(3):485–500. doi:10.1083/jcb.200702115
43. Bjorkoy G, Lamark T, Brech A, Outzen H, Perander M, Overvatn A, Stenmark H, Johansen T (2005) p62/SQSTM1 forms protein aggregates degraded by autophagy and has a protective effect on huntingtin-induced cell death. J Cell Biol 171(4):603–614. doi:10.1083/jcb.200507002
44. Tasdemir E, Maiuri MC, Galluzzi L, Vitale I, Djavaheri-Mergny M, D'Amelio M, Criollo A, Morselli E, Zhu C, Harper F, Nannmark U, Samara C, Pinton P, Vicencio JM, Carnuccio R, Moll UM, Madeo F, Paterlini-Brechot P, Rizzuto R, Szabadkai G, Pierron G, Blomgren K, Tavernarakis N, Codogno P, Cecconi F, Kroemer G (2008) Regulation of autophagy by cytoplasmic p53. Nat Cell Biol 10(6):676–687. doi:10.1038/ncb1730
45. Marino G, Ugalde AP, Salvador-Montoliu N, Varela I, Quiros PM, Cadinanos J, van der Pluijm I, Freije JM, Lopez-Otin C (2008) Premature aging in mice activates a systemic metabolic response involving autophagy induction. Hum Mol Genet 17(14):2196–2211. doi:10.1093/hmg/ddn120
46. Korolchuk VI, Mansilla A, Menzies FM, Rubinsztein DC (2009) Autophagy inhibition compromises degradation of ubiquitin-proteasome pathway substrates. Mol Cell 33(4):517–527. doi:10.1016/j.molcel.2009.01.021
47. Kimura S, Noda T, Yoshimori T (2007) Dissection of the autophagosome maturation process by a novel reporter protein, tandem fluorescent-tagged LC3. Autophagy 3(5):452–460
48. Peng H, Yang J, Li G, You Q, Han W, Li T, Gao D, Xie X, Lee BH, Du J, Hou J, Zhang T, Rao H, Huang Y, Li Q, Zeng R, Hui L, Wang H, Xia Q, Zhang X, He Y, Komatsu M, Dikic I, Finley D, Hu R (2017) Ubiquitylation of p62/sequestosome1 activates its autophagy receptor function and controls selective autophagy upon ubiquitin stress. Cell Res 27(5):657–674. doi:10.1038/cr.2017.40
49. Knaevelsrud H, Simonsen A (2010) Fighting disease by selective autophagy of aggregate-prone proteins. FEBS Lett 584(12):2635–2645. doi:10.1016/j.febslet.2010.04.041
50. Pankiv S, Clausen TH, Lamark T, Brech A, Bruun JA, Outzen H, Overvatn A, Bjorkoy G, Johansen T (2007) p62/SQSTM1 binds directly to Atg8/LC3 to facilitate degradation of ubiquitinated protein aggregates by autophagy. J Biol Chem 282(33):24131–24145. doi:10.1074/jbc.M702824200